JOURNAL OF GEOPHYSICAL RESEARCH, VOL. 107, NO. D15, 4247, 10.1029/2001JD000813, 2002

Influence of fuel sulfur on the composition of aircraft exhaust plumes: The experiments SULFUR 1–7

U. Schumann,[1] F. Arnold,[2] R. Busen,[1] J. Curtius,[2,3] B. Kärcher,[1] A. Kiendler,[2] A. Petzold,[1] H. Schlager,[1] F. Schröder,[1] and K.-H. Wohlfrom[2]

Received 7 May 2001; revised 11 November 2001; accepted 20 November 2001; published 6 August 2002.

[1] The series of SULFUR experiments was performed to determine the aerosol particle and contrail formation properties of aircraft exhaust plumes for different fuel sulfur contents (FSC, from 2 to 5500 μg/g), flight conditions, and aircraft (ATTAS, A310, A340, B707, B747, B737, DC8, DC10). This paper describes the experiments and summarizes the results obtained, including new results from SULFUR 7. The conversion fraction ε of fuel sulfur to sulfuric acid is measured in the range 0.34 to 4.5% for an older (Mk501) and 3.3 ± 1.8% for a modern engine (CFM56-3B1). For low FSC, ε is considerably smaller than what is implied by the volume of volatile particles in the exhaust. For FSC $\geq$ 100 μg/g and ε as measured, sulfuric acid is the most important precursor of volatile aerosols formed in aircraft exhaust plumes of modern engines. The aerosol measured in the plumes of various aircraft and models suggests ε to vary between 0.5 and 10% depending on the engine and its state of operation. The number of particles emitted from various subsonic aircraft engines or formed in the exhaust plume per unit mass of burned fuel varies from 2×10^{14} to 3×10^{15} kg^{-1} for nonvolatile particles (mainly black carbon or soot) and is of order 2×10^{17} kg^{-1} for volatile particles >1.5 nm at plume ages of a few seconds. Chemiions (CIs) formed in kerosene combustion are found to be quite abundant and massive. CIs contain sulfur-bearing molecules and organic matter. The concentration of CIs at engine exit is nearly 10^9 cm^{-3}. Positive and negative CIs are found with masses partially exceeding 8500 atomic mass units. The measured number of volatile particles cannot be explained with binary homogeneous nucleation theory but is strongly related to the number of CIs. The number of ice particles in young contrails is close to the number of soot particles at low FSC and increases with increasing FSC. Changes in soot particles and FSC have little impact on the threshold temperature for contrail formation (less than 0.4 K). *INDEX TERMS:* 0305 Atmospheric Composition and Structure: Aerosols and particles (0345, 4801); 0320 Atmospheric Composition and Structure: Cloud physics and chemistry; 0345 Atmospheric Composition and Structure: Pollution—urban and regional (0305); *KEYWORDS:* chemiion, sulfur, soot, contrail, aircraft, emission

1. Introduction

[2] A series of experiments (SULFUR 1–7, abbreviated as S1–S7) was performed in the years from 1994 to 1999 in order to determine the particle and contrail formation properties of aircraft exhaust plumes for different fuel sulfur content (FSC) and atmospheric conditions. This paper describes the series of experiments and summarizes the results obtained. In particular, the paper discusses the evolution of our understanding of particle formation and contrails as obtained during the course of these and related experiments.

[3] Particle and contrail formation in aircraft exhaust plumes as a function of FSC is of importance for air composition and climate [*Brasseur et al.*, 1998; *Fahey et al.*, 1999; *Schumann et al.*, 2001]. Before the first SULFUR experiment in 1994, it was hypothesized that sulfuric acid in aircraft exhaust plumes plays a strong role with respect to the number of volatile particles formed from aircraft, "activation" of soot particles as cloud condensation nuclei, and possibly "passivation" of soot for heterogeneous chemistry. These effects are important for contrail formation and air composition with possible impact on aerosols, cloudiness and climate [*Turco et al.*, 1980; *Hofmann*, 1991; *Reiner and Arnold*, 1993; *Schumann*, 1994; *Arnold et al.*, 1994]. In young exhaust plumes many small condensation nuclei (CN) were measured, but at nontypical ambient conditions (2600 m altitude, 11°C) [*Pitchford et al.*, 1991]. Soot particles were noted to hydrate when formed from fuel with high sulfur content but do not hydrate

[1]Institut für Physik der Atmosphäre, Deutsches Zentrum für Luft- und Raumfahrt, Oberpfaffenhofen, Wessling, Germany.
[2]Bereich Atmosphärenphysik, Max-Planck-Institut für Kernphysik, Heidelberg, Germany.
[3]Now at Institute for Atmospheric Physics, Johannes Gutenberg University Mainz, Mainz, Germany.

0148-0227/02/2001JD000813$09.00

otherwise [*Hallett et al.*, 1990; *Whitefield et al.*, 1993]. It was assumed that most of the fuel sulfur is burned to sulfur dioxide (SO_2) in the combustion chamber of the engine. A fraction is oxidized by reactions with co-emitted hydroxyl radicals (OH) and water to S^{VI} in form of sulfur trioxide (SO_3) and sulfuric acid (H_2SO_4) [*Miake-Lye et al.*, 1993; *Reiner and Arnold*, 1993, 1994; *Kolb et al.*, 1994]. The sulfuric acid was assumed to form liquid volatile particles by binary homogeneous nucleation [*Hofmann and Rosen*, 1978], to interact with soot [*Zhao and Turco*, 1995], and to affect contrail formation [*Kärcher et al.*, 1995]. Standard emission measurements for aircraft engines provide the smoke number (a measure for the optical blackening of a filter exposed to a given volume of exhaust gases), which may be converted with some assumptions to soot mass emissions [*Petzold et al.*, 1999], but little was known on the number, sizes and hydration properties of aviation soot from cruising aircraft [*Pitchford et al.*, 1991]. Measurements at ground behind a jet engine by *Frenzel and Arnold* [1994] showed that aircraft engines emit chemiions (CIs) formed by radical-radical reactions during the combustion process and indicated the presence of gaseous H_2SO_4. They inferred a conversion fraction ε of fuel sulfur to sulfuric acid of more than 0.4%, suggested that atomic oxygen forming during the combustion may contribute to oxidizing sulfur dioxide in addition to OH, and proposed that CIs may act as condensation nuclei for particle formation.

[4] In October 1994, particle measurements in the exhaust plume of a Concorde supersonic aircraft with the stratospheric research aircraft ER-2 revealed far larger number concentrations of small particles within aircraft exhaust plumes than expected before [*Fahey et al.*, 1995]. The emission index of non-volatile particles was derived from measurements with a condensation particle counter (CPC) [*Wilson et al.*, 1983] during three short (<20 s) plume penetrations with significant CO_2 concentration increases defining dilution at plume ages of 16–58 min. To avoid saturation effects, the ratio between total and nonvolatile particle concentration was derived from weaker plume events. From the data the amount of sulfuric acid formed in the exhaust was estimated assuming that the volatile particles were composed of sulfuric acid and water only and that the expected cutoff size (~9 nm) of the CPCs was close to the volume mean diameter of the particles. This way, a very large conversion fraction ε was derived, larger than 12%, possibly exceeding 45%. The conversion fraction predicted by models assuming zero conversion at engine exit was of order 1% [*Miake-Lye et al.*, 1994; see also *Kärcher et al.*, 1995, 1996a; *Brown et al.*, 1996a; *Tremmel et al.*, 1998]. Concurrent measurements of OH formed in the plume suggested that less than 2% of SO_2 is oxidized by OH via gas-phase reactions in the Concorde plume [*Hanisco et al.*, 1997]. New models were set up to compute the sulfur oxidation within engine combustors and turbines [*Brown et al.*, 1996b]. The models suggested ε values up to 10% for the Concorde engine. Larger values could not be excluded in view of some measurements behind conventional gas turbines [*Hunter*, 1982; *Harris*, 1990; *Farago*, 1991].

[5] Large conversion fractions would have important consequences for the impact of aircraft on air chemistry [*Weisenstein et al.*, 1996] and on contrail formation [*Miake-Lye et al.*, 1994; *Kärcher et al.*, 1996b]. The classical criterion [*Appleman*, 1953] implies contrail formation when the plume reaches liquid saturation. Even for a modest amount of fuel sulfur to sulfuric acid conversion, very large number densities of sulfuric acid droplets were computed (more than 10^{11} cm^{-3} for 0.6% conversion fraction [*Miake-Lye et al.*, 1994]). With a high amount of soot and sulfuric acid in the exhaust plume, it was conceived possible that contrails form already when reaching ice saturation, i.e., at about 3 to 4 K (increasing with altitude) higher ambient temperature than if forming at liquid saturation, which could considerably extend the atmospheric region in which contrails form [*Miake-Lye et al.*, 1993; *Schumann*, 1996a].

[6] Hence the topic was of high interest with many open questions: How many soot particles are formed per mass unit of burned fuel and how large are these soot particles? How large is the conversion fraction ε of fuel sulfur to sulfuric acid? How many CIs are emitted and how important are CIs for particle formation? How many volatile particles are formed per mass of burned fuel? What is the impact of fuel sulfur on contrail formation? How important is the FSC for volatile aerosol formation, soot activation, and contrail ice crystal formation?

[7] Therefore the series of SULFUR experiments was initiated in December 1994. New questions arising from the results of the earlier experiments and new instrument developments led to the series of experiments to be described in this paper. Many of the results of the individual experiments have been published shortly after the experiments by various teams of authors, and these papers will be cited below, but none of them gives a full account for the series of experiments performed so far. This paper gives a synopsis of the experimental conditions and the results, and it describes the sequence of understanding obtained during the development of the research in this field. The discussion includes results from related measurements performed by our group within the Pollution From Aircraft Emissions in the North Atlantic Flight Corridor (POLINAT) projects [*Schumann et al.*, 2000a] with plume measurements behind several aircraft including the NASA DC8 [*Thompson et al.*, 2000]. Also included are results of the NASA Subsonic Aircraft Contrail and Cloud Effects Special Study (SUCCESS) [*Toon and Miake-Lye*, 1998] and a series of Subsonic Assessment Near-Field Interactions Field Experiments (SNIF, I–III) [*Hunton et al.*, 2000]. Moreover, we report results obtained at ground within this series of experiments and within related projects, including modeling performed during the Chemistry and Microphysics of Contrail Formation (CHEMICON) project [*Gleitsmann and Zellner*, 1999; *Tremmel and Schumann*, 1999; *Sorokin and Mirabel*, 2001; *Starik et al.*, 2002]. Additionally, new data are reported from the most recent SULFUR 7 experiment.

2. Experiments

[8] The series of SULFUR experiments, see Table 1, was initiated by Deutsches Zentrum für Luft- und Raumfahrt, Institut für Physik der Atmosphäre (DLR, IPA), and performed in close cooperation with partners, in particular with Max-Planck-Institut für Kernphysik (MPIK), Heidelberg, to

Table 1. Summary of SULFUR Experiments

Experiment[a]	Date	Aircraft Investigated	FSC; Left/Right, μg/g	Experimental Topics; Observation Platform	Publications Describing Experiment Results
1	13 December 1994	ATTAS	2 ± 0.7/250 ± 17	visual check of threshold conditions for contrail onset; Lufthansa Piper Cheyenne	*Busen and Schumann* [1995]
2	22 March 1995	ATTAS	170 ± 10/5500 ± 100	first microphysical measurements; DLR Falcon	*Schumann et al.* [1996], *Gierens and Schumann* [1996]
3	13 July 1995	ATTAS	212/2800 ± 160	emissions at engine exit; ground	*Arnold et al.* [1998a]
4	8–15 March 1996	ATTAS; A310-300	6 ± 2/2830 ± 280; 850 ± 10/ 2700 ± 200	variation of aircraft, FSC and first near-field measurements in exhaust plumes and contrails; Falcon and ground behind ATTAS	*Petzold et al.* [1997], *Petzold and Schröder* [1998], *Petzold and Döpelheuer* [1998], *Arnold et al.* [1998b], *Schröder et al.* [2000a]
5	14–18 April 1997	ATTAS	22 ± 2/2700 ± 350	first measurements of sulfuric acid, chemiions, volatile and non-volatile aerosols within and outside contrails, soot impact on ice particles, emissions of hydrocarbons and carbon monoxide; Falcon and ground	*Curtius et al.* [1998], *Schröder et al.* [1998], *Arnold et al.* [1999], *Slemr et al.* [1998, 2001]
P	3 July 1995, 24 September 1997, 23 October 1997	B747, DC10, B747, A340-300, DC8	240, 265, 260, 480, 690	wide-body aircraft plume particles and gaseous emissions, intercomparison between Falcon, A340 and DC8, gaseous sulfuric acid from the DC8; Falcon	*Schulte et al.* [1997], *Konopka et al.* [1997], *Tremmel et al.* [1998], *Helten et al.* [1999], *Schumann et al.* [2000a]
6	28–30 September 1998	ATTAS; B737-300	2.6 ± 0.3/118 ± 12; 2.6 ± 0.3/56 ± 6; 2.6 and 66 at ground	first detailed resolution of nuclei mode size range by 8–9 particle counters with 3–60 nm cutoff sizes, for two aircraft, and sulfuric acid and ion concentrations; Falcon and ground behind ATTAS	*Petzold et al.* [1999], *Schröder et al.* [2000b], *Arnold et al.* [2000], *Curtius et al.* [2002], *Brock et al.* [2000], *Wohlfrom et al.* [2000]
7	15 September 1999	A340-300; B707-307C	120 ± 12; 380 ± 25	test of impact of engine efficiency and measurements of aerosol and large ion clusters in young plumes (0.25–1 s); Falcon	*Schumann* [2000], *Schumann et al.* [2000b], this work

[a]Numbers including "P" for POLINAT.

investigate particle formation from various aircraft, burning fuels with different FSCs during the same flight. The experiments S1–S7 included 10 flights with measurements in the young exhaust plume of various aircraft at separation distances varying from 25 m to about 5 km (plume ages 0.15–30 s, see Figure 1a, for example), and measurements at ground during S3 to S6. The measurements inside and outside of aircraft plumes have been performed on board the Falcon aircraft of DLR, see Figure 1b. Ground experiments were performed to measure particles and particle precursors close to jet engine exit.

[9] The observations have been performed with an increasingly refined set of instruments by various partners, see Table 2, as described in detail in the individual papers listed. The instruments include innovative methods, such as four different mass-spectrometer instruments of MPIK, and a system of instruments to measure the number, size and volatility of aerosols in the diameter range from 3 nm to 20 μm of DLR-IPA and partners.

[10] In most of the experiments the DLR Advanced Technology Testing Aircraft System (ATTAS) was used as the aircraft causing the exhaust, see Table 3. The ATTAS is a midsized two-engine jet aircraft of type VFW 614, with Rolls-Royce SNECMA M45H Mk501 engines, see Figure 1c, built in 1971 [*Busen and Schumann*, 1995]. In more recent experiments, also younger and larger jet aircraft were investigated; their engines have higher thrust, bypass ratio, and pressure ratio. Higher bypass engines offer higher overall propulsion efficiency causing less waste heat released into the plume gases [*Cumpsty*, 1997], which impacts contrail formation [*Schumann*, 1996a, 2000]. The fuel sulfur conversion fraction depends probably on combustion pressure [*Brown et al.*, 1996b], which increases with the pressure ratio.

[11] The experiments cover a wide range of FSC values. Aviation fuels are produced with FSC values from near 1 μg/g to an upper limit of 3000 μg/g. The median FSC value of fuels provided for airliners is near 400 μg/g [*IPCC*, 1999]. In cases S1, S6, and S7 the FSC was varied by using different fuel deliveries. In cases S2–S5, up to 60 kg of dibuthylsulfide ($C_8H_{18}S$) containing a 22% mass fraction of sulfur were added to one of the fuel tanks to increase the FSC relative to the fuel in other tanks to the desired level. The melting-, boiling-, and flame-point temperatures and the density of the additive (−80°C, 182°C, 62°C, 840 kg m^{-3}) are sufficiently similar to those of standard Jet-A1 kerosene fuel (−50°C, 164 to 255°C, 52°C, 800 kg m^{-3}) to allow for reasonable mixing, and the additive can be handled easily. Later, other experimenters used tetrahydrothiophene (C_4H_8S; −96°C, 120°C, 12°C, 1000 kg m^{-3}) for

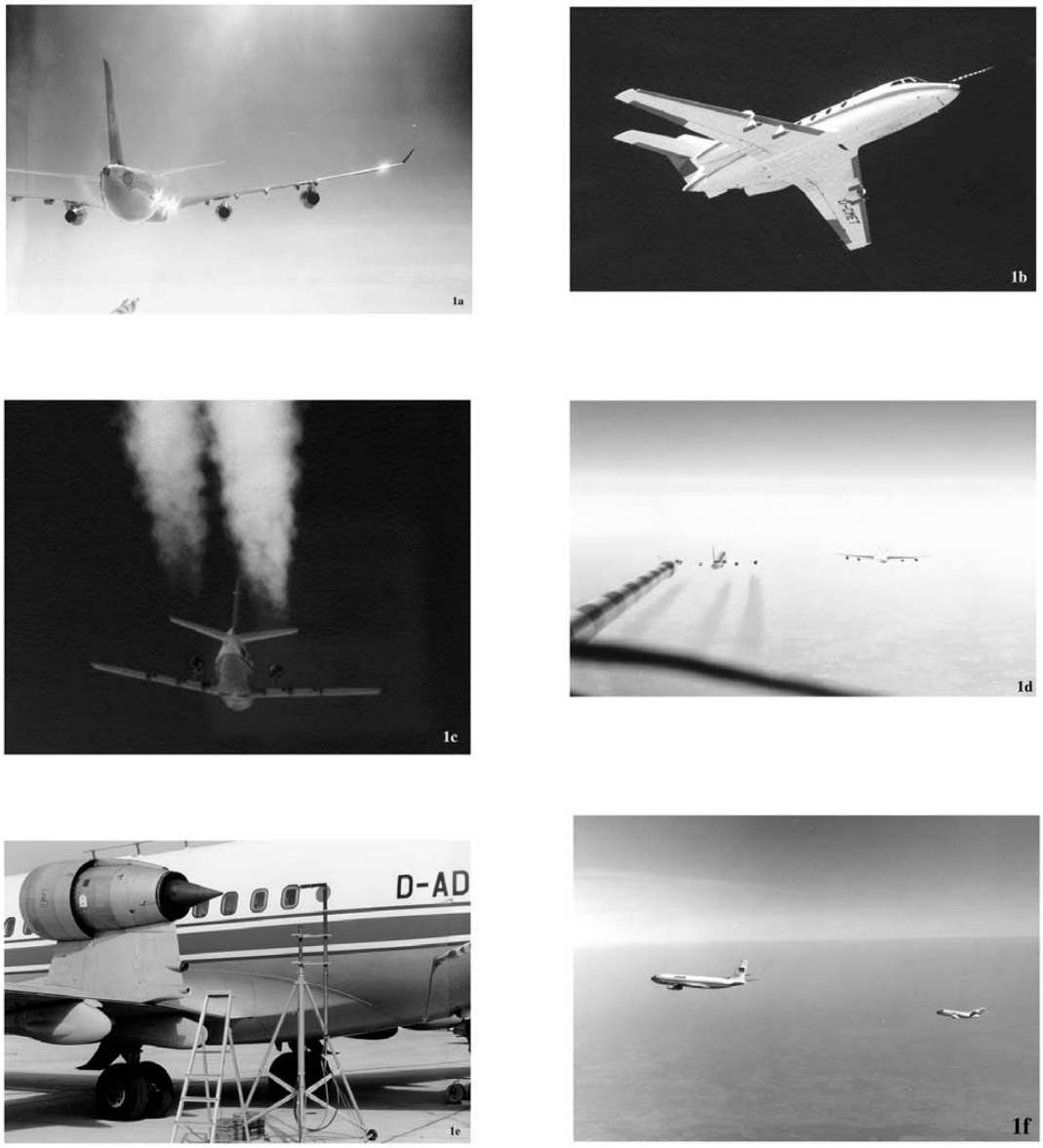

Figure 1. (a) Photo of the Airbus A340 at cruise during S7 measuring about 70 m behind the right turbofans. The nose boom of the Falcon used for turbulence measurements is visible at the lower edge of the photo; (b) the Falcon with particle measurement systems below the wing and aerosol inlet at top of the fuselage during S4; (c) the ATTAS at cruise during S2 burning low (high) fuel sulfur content on left (right) engine; (d) the A340 and the B707, wing by wing, one with, the other without contrails during S7; (e) sample inlet behind the ATTAS engines at ground during S3; (f) Falcon measuring in the B707 plume 70 m behind the engines during S7. See color version of this figure at back of this issue.

this purpose [*Cofer et al.*, 1998; *Miake-Lye et al.*, 1998] which shows larger differences to kerosene. The FSC was analyzed from fuel samples with standard laboratory methods or inferred from the amount of sulfur added to a reference fuel. The reproducibility of sulfur analysis from the same sample in various laboratories with 95% confidence interval is better than 10% [*Schröder et al.*, 2000b]. Larger differences (maximum of 25%, S5) were found

Table 2. Instruments Used in the Various Experiments

Instrument	Measured Parameter	Method	S1	S2	S3	S4	S5	P	S6	S7	Operator[a]	Reference
Video, photos, cockpit instruments on Falcon	contrail onset, flight level, speed	standard instruments of the Falcon (S1: Piper Cheyenne IIIA)	X	X	X	X	X	X	X	X	DLR	*Schumann et al.* [1996]
PT100 and PT500	temperature	standard instrumentation of the Falcon		X	X	X	X	X	X	X	DLR	*Schumann et al.* [1996]
Five-hole pressure transducer, horizontal position	pressure, turbulent wind components, position	standard instrumentation of the Falcon		X	X	X	X	X	X	X	DLR	*Bögel and Baumann* [1991]
Vaisala HMP35	H_2O, relative humidity	capacitive polymer humicap-H		X		X	X	X	X	X	DLR	*Ström et al.* [1994]
Lyman-alpha hygrometer	H_2O, mixing ratio	Buck research hygrometer		X							DLR	*Ström et al.* [1994]
Frost point	H_2O, frost point	frost point mirror, Buck					X		X	X	DLR	*Busen and Buck* [1995]
CPC	condensation nuclei (CN), particle concentration with $d >$ 7 nm, $d >$ 18 nm	modified TSI 3760, condensation particle counters (CPCs), interstitial aerosol inlet		X		X					University of Stockholm	*Schumann et al.* [1996]
CPC	$d >$ 5, 10, 14 nm volatile and nonvolatile aerosols ($d >$ 14 nm for S5, $d >$ 10 nm for S6 and S7)	modified TSI 3760A and 3010 CPCs with interstitial aerosol inlet, operated with heated sample (in S5 alternatively)				X	X		X	X	DLR	*Petzold et al.* [1997]
CPC	$d >$ 3 nm	ultrafine CPC, modified TSI 3025, interstitial aerosol inlet							X		DLR	*Schröder et al.* [1998]
N-MASS	number concentration for particles with $d >$ 4, 8, 13, 30, 55 nm	CN counter cascade							X		University of Denver	*Brock et al.* [2000]
PCASP	dry aerosol size distribution, 0.1 $< d <$ 1 μm, 32 channel resolution (20 used)	PMS passive cavity aerosol spectrometer probe, PCASP-100, internal, interstitial aerosol inlet		X							University of Stockholm	*Schröder and Ström* [1997]
PCASP	dry aerosol size distribution, 0.1 $< d <$ 3 μm, 15 channel resolution	PMS PCASP-100, wing station				X	X		X	X	DLR	*Schröder and Ström* [1997]
FSSP 100	cloud element size distribution, 1 μm $< d <$ 16 μm	forward scattering spectrometer probe (FSSP), Particle Measurement Systems (PMS)		X							DLR	
FSSP-300	aerosol and cloud size distribution, 0.35 μm $< d <$ 20 μm	FSSP, PMS				X	X		X	X	DLR, S4: University of Mainz	*Schröder et al.* [2000a, 2000b], *Borrmann et al.* [2000]
PSAP	integral soot mass, absorption coefficient	soot photometer, filter deposition technique					X		X		DLR	*Petzold et al.* [1999]
MASP	aerosols sizes and forward/backward scattering ratio, 0.4 μm $< d <$ 10 μm	multiangle scattering spectrometer probe				X					DLR and NCAR	*Kuhn et al.* [1998]
MASS	size distribution, ~12 nm $< d <$ 0.4 μm	Mobile Aerosol Sampling System			(X)	X		X			UMR	*Hagen et al.* [1996]
Integrating Nephelometer	scattering coefficient	integrating volume scattering technique					X		X		DLR	*Petzold et al.* [1999]

Table 2. (continued)

Instrument	Measured Parameter	Method	S1	S2	S3	S4	S5	P	S6	S7	Operator[a]	Reference
CIMS	trace gases SO_2, HONO, HNO_3	Chemi Ionization Mass Spectrometry						X				*Arnold et al.* [1992, 1994]
SIOMAS	small chemiions (1–220 in S3; 1–450 amu in S4 and S5)	Small Ion-Mass Spectrometer			X	X	X				MPIK	*Arnold et al.* [1998a, 1998b]
LIOMAS	large positive and negative chemiions (1–8500 amu)	Large Ion-Mass Spectrometer						X	X	(X)	MPIK	*Wohlfrom et al.* [2000]
VACA	total (gaseous and evaporated liquid) H_2SO_4	Volatile Aerosols Component Analyzer: CIMS with NO_3^- ions and heated inlet					X		X		MPIK	*Curtius et al.* [1998], *Curtius and Arnold* [2001]
Gerdien condenser	positive total ion concentration	electrostatic probe								X	MPIK	*Arnold et al.* [2000]
NDIR CO_2 sensor	carbon dioxide (CO_2) concentration	nondispersive infrared differential absorption					(X)	X	X		DLR	*Schulte et al.* [1997]
GPS	distance	Differential Global Positioning System					X	(X)	(X)		DLR	
Grab samples	NMHC concentration	grab samples analyzed for hydrocarbons and CO by gas chromatography					X				FhG/IFU	*Slemr et al.* [2001]
VUV fluorescence CO	carbon monoxide (CO) concentration	vacuum ultraviolet fluorescence								X	DLR	*Gerbig et al.* [1996]
Emission measurement system	EI of CO_2, CO, HC, NO_x, NO, soot smoke number (SN)	ICAO standardized instruments			X						MTU	*ICAO* [1981]

[a]DLR, Deutsches Zentrum für Luft- und Raumfahrt, Oberpfaffenhofen; FhG/IFU: Fraunhofer-Institut für Atmosphärische Umweltforschung, Garmisch-Partenkirchen; MPIK: Max-Planck-Institut für Kernphysik, Atmospheric Physics Division, Heidelberg; MTU: Motoren und Triebwerk Union, München; NCAR: National Center for Atmospheric Research, Boulder, Colorado; UMR: University of Missouri-Rolla, Rolla, Missouri Entries with parentheses (X) denote instrument applications with reduced data output.

Table 3. Aircraft and Engines Investigated

Aircraft	Engine	Year[a]	Bypass Ratio	Pressure Ratio	Thrust, kN	Experiment
B707-307C	PW JT3D-3B	1968	1.4	13.6	80.1	S7
ATTAS	Mk501	1971	3.0	16.5	32.4	S1–S6
B747-200B	JT9D-7J	1971, 1976	5.1	23.5	222.4	POLINAT
DC10-30	CF6-50C	1974	4.3	27.8	224.2	POLINAT
B737-300	CFM56-3B1	1987	5.1	22.4	89.4	S6
A310-300	CF6-80C2A2	1991	5.1	28	233.3	S4
A340-300	CFM56-5C2	1993	6.8	28.8	138.8	POLINAT
DC8	CFM56-2C1	1994	6.0	~23.5	~97.9	POLINAT
A340-300	CFM56-5C4	1998	6.6	31.1	151.2	S7

[a]The year is the year of engine construction; the bypass ratio is the ratio of the mass flux through the outer fan duct of the engine relative to the mass flux through the core duct of the engine at takeoff; the pressure ratio is the ratio between pressure at combustor inlet and at engine inlet at takeoff; the thrust is given for takeoff [*ICAO*, 1995].

between FSC analysis of fuel samples and FSC values derived from the amount of sulfur added, possibly due to incomplete mixing and partial evaporation of the additive. For the two B747 aircraft and the DC10 during POLINAT the FSC is determined from SO_2 and CO_2 measurements in the plume with about 30% accuracy [*Arnold et al.*, 1994; *Schulte et al.*, 1997; *Schumann et al.*, 2000a].

[12] Table 4 lists the parameters during the flight measurements reported. The aircraft were operated mainly in the upper troposphere, with or without contrails or at threshold

Table 4. Atmospheric Conditions During the In-Flight Measurements

Experiment[a]	Aircraft, Case	Date	FL, hft	FSC,[b] μg g^{-1}	p, hPa	T, °C	RH, %	V, m s^{-1}	η	T_c,[c] °C	Contrail Seen
S1	ATTAS	13.12.94	299	2, 250	302.3	−49.7	44	115	0.14	−49.6	threshold
S2	ATTAS, C1	22.3.95	288	170, 5500	317	−49.0	42	163	0.172	−48.8	threshold
	C2		290	170, 5500	316	−49.5	36	163	0.175	−49.1	threshold
	C3		290	170, 5500	315	−49.2	37	163	0.182	−49.3	threshold
	C4		290	170, 5500	316	−48.3	37	163	0.198	−48.8	threshold
	low/high		310	170, 5500	287	−55	40	163	0.168	−50	yes
	high/high		300	5500	301	−51.3	45	163	0.171	−50	yes
S4	ATTAS	12.3.96	240	6, 2830	392.7	−39	10	160	0.17	−48.3	no
			310	6, 2830	287.4	−43	20	175	0.17	−50.9	no
	A310	13.3.96	350	850, 2700	238.4	−58	15	180	0.28	−51.6	yes
	ATTAS	15.3.96	310	6, 2830	287.4	−52.3	40	165	0.17	−50.1	yes
			270	6, 2830	344.3	−42	45	160	0.17	−48.1	no
S5	ATTAS	16.4.97	250	22	376	−44	30	160	0.17	−48.0	no
	H_2SO_4 inject.		310	22	287	−52	45	160	0.17	−49.9	yes
	ATTAS	18.4.97	260	24, 2700	360	−42	50–65	160	0.17	−46.4	no
			310	24, 2700	287	−54	90–65	165	0.17	−48.7	yes
P	B747-200B	3.7.95	330	240	262	−46	17	257	0.33	−49.7	no
	DC10-30	3.7.95	330	265	262	−45	18	255	0.33	−49.7	no
	B747-200B	3.7.95	330	260	262	−45	21	255	0.33	−49.6	no
	A340-300	24.9.97	350	480	238.4	−51	29	200	0.3	−50.1	yes
	DC8	23.10.97	330	690	261	−49	57	227	0.3	−47.8	yes
S6	ATTAS	28.9.98	260	2.6, 118	359	−38	35–40	153	0.17	−47.9	no
			320	2.6, 118	274	−52	35–50	177	0.17	−50.8	yes
	B737	30.9.98	190	2.6, 56	490	−14	75–85	141	0.3	−39.5	no
			260	2.6, 56	360	−30	55–65	167	0.3	−44.7	no
			350	2.6, 56	238	−52	>60	192	0.3	−49.2	yes
			370	2.6, 56	216	−56	>65	199	0.3	−49.8	yes
S7	B707	15.9.99	310	120	288	−42	20	187	0.25	−50.0	no
			334	120	256.05	−49.3	38	190	0.31	−49.4	threshold
	A340		336.6	380	252.34	... 50.42	42	195	0.23	−50.6	threshold
			349	380	245.32	−50.9	34	209	0.24	−51.0	threshold
	B707		342	120	247.65	... 50.54	33	203	0.28	−50.4	threshold
	A340		314	380	281	−42	20	194	0.27	−50.0	no

[a]Experiment name, date, flight level (FL, 1 hft = 100 feet = 30.48 m), fuel sulfur content (FSC), ambient pressure (p), temperature (T), relative humidity of liquid saturation (RH), true air speed V, overall propulsion efficiency η, computed contrail threshold temperature (T_c), and report on whether a contrail was seen or not.

[b]The fuel analyses (~20 samples) imply a combustion heat $Q = 43.21 \pm 0.06$ MJ kg^{-1}, and a hydrogen mass fraction of 13.71 ± 0.1% ($EI_{H2O} = 1.225 \pm 0.01$; $EI_{CO2} = 3.16 \pm 0.005$).

[c]T_c is computed for the measured fuel properties and the estimated overall propulsion efficiency η using the Schmidt/Appleman criterion with code available from http://www.op.dlr.de/ipa/schumann/.

conditions where contrails were just forming or disappearing. Some of the chased fast aircraft were operated at reduced power settings to let the slower Falcon follow at close distance.

3. Results

3.1. Visual Observation of Contrail Formation Independent of FSC During SULFUR 1

[13] As a test for postulated influences of sulfur emissions on nucleation, the contrail formation from the ATTAS was investigated using fuels with different FSCs (2 and 250 μg/g) on the two engines during the same flight [*Busen and Schumann*, 1995]. Contrail formation was observed visually from another aircraft following at close distance and documented in photos and videos. Ambient temperature and humidity were deduced from a nearby radiosonde at flight level. At threshold conditions, short contrails were seen to form about 30 m behind the engines. Other than expected from previous discussions on the importance of fuel sulfur for particle formation, the observations, photos and videos revealed no systematic difference in the contrails forming from the two engines.

[14] However, the contrail did form at a temperature that was about 2 K warmer than expected from the Appleman criterion. This difference is not caused by sulfur emissions but by effects of the overall propulsion efficiency η not included in the Appleman criterion [*Busen and Schumann*, 1995]. The higher the value of η, the less combustion heat leaves the engine exit with the exhaust, allowing contrails to form at higher ambient temperature [*Schmidt*, 1941]. The value of $\eta = VF/(Q\ m_f)$ depends on the aircraft speed V, thrust F, specific fuel combustion heat Q, and fuel consumption rate m_f [*Schumann*, 1996a]. With $(1\text{-}\eta)\ Q$ as effective combustion heat, the Schmidt/Appleman criterion fits the observed threshold temperatures for contrail formation to better than 0.5 K (see Table 4).

[15] The threshold temperature is computed assuming that heat and water vapor in the exhaust are well mixed when leaving the engine and that the plume reaches liquid saturation locally during mixing. However, water is emitted only from the core engine while heat is emitted from both the core and the bypass of the engine, implying nonuniform exit conditions. Moreover, part of the combustion heat leaves the engine with the jet as kinetic energy and is dissipated to heat during mixing of the jet with ambient air [*Schumann*, 1996a]. Therefore the humidity in the plume deviates slightly from what is expected according to the Schmidt/Appleman concept. A model computation for the S1 conditions revealed a local liquid water supersaturation of about 7%, enough to let fresh soot particles larger than 30 nm diameter become activated and form water droplets even at threshold conditions [*Schumann et al.*, 1997]. If soot would be hydrated before reaching liquid saturation, contrails could form at slightly higher ambient temperature [*Kärcher et al.*, 1996b]; a 10% lower critical humidity increases the threshold temperature, which is typically below −40°C, by 0.9 to 1.1 K. The liquid droplets formed freeze quickly and then grow further by water deposition because of high ice supersaturation. Homogeneously nucleated sulfuric acid droplets do not freeze and grow fast enough under threshold conditions to form a visible contrail [*Kärcher et al.*, 1995]. The number of ice particles formed must be larger than 10^4 cm^{-3} in order to produce a visible contrail as early as observed [*Kärcher et al.*, 1996b]. The water droplets freeze at timescales of the order of milliseconds and the accommodation coefficient of water vapor molecules on the ice surface is at least 0.2 to allow for particle growth as fast as observed in this experiment [*Schumann*, 1996b].

3.2. Discovery of Fuel Sulfur Influence on Particle Formation During SULFUR 2

[16] The S2 experiment was performed to cover larger FSC values and to measure the properties of particles formed as a function of FSC [*Schumann et al.*, 1996]. Again, the ATTAS aircraft was used as exhaust forming aircraft. Different FSC values of 170 and 5500 μg/g were prepared by using a standard fuel with 170 μg/g in one aircraft fuel tank and by adding dibuthylsulfide to the fuel in the other tank. Besides photo and video observations from close distance, in situ measurements were made flying the Falcon aircraft in the wake of the ATTAS at plume ages of about 20 s, at altitudes between 9 and 9.5 km, and temperatures between −49° and −55°C, when the visible contrail extended to about 2 km length.

[17] Besides standard instruments available on the Falcon, the instruments (see Table 2) included two CPCs with cutoff sizes of 7 and 18 nm, and a Passive Cavity Aerosol Spectrometer Probe (PCASP) counting optically the dried aerosol larger 120 nm in diameter after entering the measurement systems inside the aircraft via an "interstitial," i.e., backward facing sample inlet at top of the fuselage outside the boundary layer, and a Forward Scattering Spectrometer Probe (FSSP-100) of Particle Measurement Systems Inc. (PMS) mounted outside the aircraft at a wing station for particles larger than 1 μm.

[18] The observations demonstrated that fuel sulfur emissions do cause measurable and even visible changes in the particle properties and contrails. At ambient temperatures 5 K cooler than the threshold temperature for contrail onset, the plume was visible already about 10 m behind the engine exit for high FSC, but 15 m behind the engine exit for low FSC (see Figure 1c). During descent through the level of contrail onset the high sulfur contrail remained visible at slightly lower altitude (25 to 50 m) or higher temperature (0.2 to 0.4 K). The higher FSC caused a larger optical thickness of the contrail shortly after onset. The high FSC contrail grew more quickly but also evaporated earlier than the low FSC contrail. At plume ages of about 20 s each engine plume was spread to about 20 m diameter. The plumes contained many subvisible particles. Peak number densities were 30,000 cm^{-3} for particles of diameter above 7 nm and 15,000 cm^{-3} above 18 nm. The particle measurements at low FSC indicate that the number of particles larger than 7 nm measured in the plume originated mainly from emitted soot particles. The number of particles in this size range increases by about 25% for particle of diameter above 7 nm and by 50% for particles above 18 nm when the FSC is increased by a factor of 30. The results suggest that part of the fuel sulfur is converted to sulfuric acid which interacts with the soot. Hence sulfuric acid tends to "activate" soot particles [*Kärcher et al.*, 1996b]. Estimates of the number, size, and volume of the particles reveal that the measurements are consistent with estimated soot emission indices (EIs) and some volatile material from sulfur to

Table 5. Emission Parameters of the ATTAS Engines at Ground and at Cruise

			Ground,[b] power, %						
Parameter[a]	Unit	Origin	7	18.5	30	57.5	85	100	Cruise (Origin)
EI_{NOx}	$g(NO_2)\ kg^{-1}$	MTU	1.9	3.0	4.1	6.7			5–9[c]
		ICAO	1.5		3.6		9.3	11.5	
EI_{NO}	$g(NO_2)\ kg^{-1}$	MTU	1.0	1.2	2.1	4.0			0.8–1.5[c]
		IFU	<1.9	<1.7	<2.1		3.9		
		DLR		0.1	1		3.4		
EI_{CO}	$g\ kg^{-1}$	MTU	112.	52.	24.	6.			12–22[d]
		ICAO	178.		51.		7.9	6.2	
		IFU	125	59	26		5.6		
		DLR	104	50	22		4.8		
EI_{HC}	$g\ kg^{-1}$	MTU	31.	6.	2.	0.4			0.02–0.25[d]
		ICAO	59.5		7.4		0.74	0.75	
EI_{soot}	$g\ kg^{-1}$	DLR	0.013	0.045	0.13		0.4		0.1–0.15[e]
SN		MTU	2	5	10	24			
		ICAO	2.7		10.9		38.4	46.3	
m_f	$kg\ s^{-1}$	MTU	0.054	0.099	0.146	0.270			0.12[f]
		ICAO	0.053		0.146		0.416	0.498	0.22[d]
T_C	K	RR	678		683		746	760	617[f]
T_B	K	RR	293		293		292	295	237.5[f]
T	K	IFU	561	585	615		647		620–655[c]
		DLR	586	605	635		668		
V_C	$m\ s^{-1}$	RR	80		172		357	414	417[f]
V_B	$m\ s^{-1}$	RR	96		180		274	290	248.2[f]

[a]Emission indices (EIs) for nitrogen oxides (NO_x) and nitric oxide (NO, in mass units of NO_2) for carbon monoxide (CO) and for nonmethane hydrocarbons (HC, in mass units of CH_4); smoke number (SN); fuel flow rate (m_f); core exit static temperature (T_C); bypass exit static temperature (T_B); gas static temperature (T) measured 1.8 m past engine nozzle exit; core exit jet speed (V_C), bypass exit speed (V_B), for various power settings in percent of full power at ground and for observed cruise conditions.

[b]Ground measurements during SULFUR 3 and 4 behind the ATTAS by Motoren and Triebwerk Union (MTU, G. Huster, personal communication, 1995) from measurements reported in the ICAO emission database [*ICAO*, 1995] and from FTIR emission spectrometry by Fraunhofer-Institut für Atmosphärische Umweltforschung (IFU) [*Heland and Schäfer*, 1998; J. Heland, personal communication, 1996] and by *Haschberger et al.* [1997] (DLR); and as derived from engine performance data provided by Rolls-Royce (RR). The MTU values are mean values over three measurements: One from the right wing engine with low FSC (218 μg/g), one from the left wing engine with low FSC (218 μg/g), and one from the left wing engine with high FSC (2800 μg/g), without significant differences and with relative deviations of a few percent.

[c]*Haschberger and Lindermeir* [1997].

[d]Range of data for various plume encounters from *Slemr et al.* [2001].

[e]*Petzold and Döpelheuer* [1998].

[f]Engine computations for conditions of S1; for S2, see *Schumann et al.* [1996].

sulfuric acid conversion at a fraction ε of about 0.4% or little larger, as suggested by *Frenzel and Arnold* [1994]. Color differences were observed between contrails formed from two engines burning fuels with different FSC and this color difference can be explained with more but smaller ice particles for higher FSC [*Gierens and Schumann*, 1996].

[19] The results of S1 and S2 were used to guide and test model studies in many follow-up papers [*Kärcher*, 1996, 1998a, 1998b; *Kärcher et al.*, 1996b, 1998a; *Brown et al.*, 1996b, 1997; *Gleitsmann and Zellner*, 1998a, 1998b, 1999; *Konopka and Vogelsberger*, 1997; *Andronache and Chameides*, 1997, 1998; *Taleb et al.*, 1997; *Lukachko et al.*, 1998; *Yu and Turco*, 1997, 1998a; *Jensen et al.*, 1998a, 1998b; *Garnier and Laverdant*, 1999; *Tremmel and Schumann*, 1999; *Zaichik et al.*, 2000; *Starik et al.*, 2002]. In particular, *Yu and Turco* [1998a] showed that the measurements can be quantitatively reproduced to good approximation with a plume aerosol model assuming ε = 1.8%, when including enhanced coagulation by CIs in the model. The relatively strong increase of the observed number of particles >18 nm compared to that >7 nm is caused by scavenging of vapors and particles by ice particles in the young contrail which then leave the aerosol measured after evaporation. The remaining sulfate aerosol accumulation mode may contribute to cloud condensation and ice nuclei. The observations and the model studies show that the FSC does not influence the threshold temperature for contrail formation but does influence the optical appearance of the contrail. An increase in FSC is likely to cause more sulfuric acid in the plume and by a combination of homogeneous and soot-induced heterogeneous freezing more particles which grow by water uptake, freeze, and form ice particles [*Kärcher et al.*, 1998a].

3.3. Ground-Based Gaseous and Ion Emission Measurements During SULFUR 3

[20] A ground-based experiment was performed to insure that the differences measured between the left and right engine exhaust plumes originate from different FSC and are not caused by engine differences. Moreover, this experiment was used for emission measurements very close to the engine exit, including the first mass spectrometric measurements of negative and positive CIs, and of gaseous H_2SO_4 and SO_3 in the exhaust at plume ages of 6 to 20 ms [*Arnold et al.*, 1998a]. Similar measurements were also performed behind a JT9D-7 engine in the jet-engine testing facility of Lufthansa at Hamburg at 18.6 m distance, 170 ms plume age [*Arnold et al.*, 2000].

[21] The EIs of NO, NO_x, CO, HC, and the smoke number of the ATTAS engines were measured at ground using instruments satisfying International Civil Aviation Organization (ICAO) standards [*ICAO*, 1981]. The samples were taken behind the ATTAS at the same position (centerline, 1 m behind engine exit cone, 1.8 m behind engine nozzle exit, see Figure 1e) for various power settings and

FSC values, see Table 5. The measured values show the same trends with power as the ICAO data but with 20% higher EIs for NO_x and about 50% lower values for CO and HC compared to the values reported by *ICAO* [1995]. The lower EI_{CO} values are also supported by simultaneous Fourier transform infrared spectrometer (FTIR) measurements performed during S4 at ground and in flight [*Haschberger et al.*, 1997; *Heland and Schäfer*, 1998]. *ICAO* [1995] contains no information on the NO/NO_x ratio. The measurements indicate that about 30 to 50% of the NO_x is emitted as NO_2; smaller values have been derived during cruise from FTIR measurements (NO_2/NO_x ratio of 12–22%) [*Haschberger and Lindermeir*, 1997]. Anyway, the NO_2/NO_x fraction measured for the ATTAS is far higher than for the RB211-524 engine [*Schumann*, 1995], which emits less than 5% of all NO_x as NO_2, possibly due to higher combustion temperature and pressure. The emission data obtained behind the left and right wing engine of the ATTAS, and for different FSC values (with different amounts of additives), show no significant differences. Hence any difference measured in the plumes is not caused by engine differences. Moreover, the FSC has no detectable influence on the emission index values listed, including the smoke number. The basic emissions including soot seem to be invariant to FSC. These measurements have been used for comparison to in-flight measurements of EIs of CO and HC by *Slemr et al.* [1998, 2001]. As a result, the ATTAS engine is one of the best characterized engines described in the open literature, well suited for modeling.

[22] Mass spectra of negative and positive CIs were measured using a quadrupole Ion Mass Spectrometer (IOMAS). Gaseous H_2SO_4 and SO_3 were measured using a Chemical Ionization Mass Spectrometer (CIMS). For these measurements the exhaust is passed through a flow tube system containing a capillary ion source. The source introduces nitrate-ions (mostly $NO_3^-(HNO_2)_n$, $n = 0, 1, 2$) into the flow tube which react with gaseous H_2SO_4 and SO_3 present in the exhaust to form HSO_4^- ions and NO_3^- SO_3^- ions, respectively. Analyzing the ion composition in the flow tube downstream of the source, the number density of H_2SO_4 and SO_3 can be determined for given reaction time and rate coefficients of the respective ion-molecule reactions. The results show a total negative ion concentration of more than 1.4×10^7 cm^{-3} at plume ages of around 10 ms in the exhaust of a jet engine at the ground [*Arnold et al.*, 1998a]. For low FSC the S^{VI} concentration was measured implying a conversion fraction ε of 1.2%. For high FSC most of the sulfuric acid formed ions $HSO_4^-(H_2SO_4)_m$ with $m > 1$ with masses outside the range detectable by the IOMAS instrument (220 atomic mass units, amu). This finding initiated new experiments using mass spectrometers with larger mass ranges as described below.

3.4. Comparison of Exhaust From Different Aircraft During SULFUR 4

[23] In order to generalize the results to other aircraft, with more modern engines, and to search for sulfuric acid in the exhaust plume of cruising aircraft, an experiment was organized in which the Falcon could measure in the young exhaust plume of an Airbus A310 at cruise (plume ages 1–4 s), and behind the ATTAS with refined instruments, at very close approach (plume age 0.5–1 s), for situations with and without contrail formation and for a large range of FSC values (6 to 2830 μg/g) [*Petzold et al.*, 1997]. The close approach of the Falcon to the ATTAS and Airbus aircraft was made possible by the Falcon pilots after learning about the nature of wake vortex formation [*Gerz and Holzäpfel*, 1999]. Steady flight conditions could be reached at some positions within the wake vortex as close as 25 m (during S6) behind the leading aircraft by expert pilots. Steady flight is not possible at plume ages of about 5 to 20 s when the wake vortices are fully developed and break up into small-scale turbulence [*Gerz et al.*, 1998; *Holzäpfel et al.*, 2001].

[24] During S4, new PMS-type optical spectrometers were implemented: A PCASP-100 (0.1–3 μm dry diameter) and a FSSP-300 (0.35–20 μm), both mounted outside the Falcon fuselage. For the first time the spectral distribution and variability of larger aerosol and contrail ice crystals in young exhaust plumes have been documented. The ice crystal mean mode was located around 1 μm. The particle size distributions exhibit strong variations from the plume center to the diluted plume edge. The number of ice particles in the contrails were found to increase by about a factor 1.3 to 2.7 with contrail age. At 10 s plume age the number of detected particles with size >10 nm increases by a factor of 1.3 for an increase of FSC by a factor of 500.

[25] No systematic difference was found at lower plume ages (<3.3 s) in the A310 for different FSC values. However, the FSSP-300 was originally designed for low to moderate aerosol particle concentrations with corrections becoming necessary above typically 500 cm^{-3}. Hence the number of ice particles was underestimated in S4 by more than a factor of 2 [*Schröder et al.*, 2000a], leaving the possibility for a stronger sensitivity of crystal concentrations to FSC.

[26] The soot (black carbon) EI of the ATTAS engines was determined from soot size spectra measured at ground and during flight. Converted to cruise conditions with about 50% of full power, the soot mass EI amounts to 0.15 g kg^{-1} [*Petzold and Döpelheuer*, 1998]. Before these measurements, a larger EI was expected (about 0.5 g kg^{-1} [*Schumann et al.*, 1996]). Measurements of the refractive index of ice particles were found to be consistent with a large fraction of soot entering the ice particles [*Kuhn et al.*, 1998]. This was confirmed by ice crystal residuum analysis [*Petzold et al.*, 1998]. Soot collected on filters sampled at ground closely behind the engines contained sulfate. Ion chromatography measurements indicated 0.5% conversion of fuel sulfur to sulfate in the soot, with only a slight dependence on engine power setting. Organic carbon was found to contribute up to 40% to the carbonaceous fraction of soot particles at typical cruise conditions [*Petzold and Schröder*, 1998].

[27] Negative ions observed with the Small Ion-Mass Spectrometer (SIOMAS, an improved version of IOMAS) inside the plume of an Airbus A310 aircraft in flight at altitudes around 10.4 km at plume ages of about 2–3 s were mainly $HSO_4^-(H_2SO_4)_m$, $HSO_4^-(HNO_3)_m$, and $NO_3^-(HNO_3)_m$ ions with $m \leq 2$ [*Arnold et al.*, 1998b]. No negative CIs from the engine were found. It seems that the negative CIs grow rapidly, reaching mass numbers greater than measured (1100 amu) at a plume age of 3 s. The upper limit for the mean positive CI concentration estimated on the base of the measurements was about 3 ×

$10^5 - 3 \times 10^6$ cm^{-3}. This number is very close to the maximum possible ion concentration allowed by ion-ion recombination processes in the young exhaust plume. Dilution alone [*Schumann et al.*, 1998] implies about 300 times larger concentrations at engine exit.

[28] These measurements did not detect gaseous H_2SO_4 [*Arnold et al.*, 1998b; *Petzold et al.*, 1997]. Only an upper limit for the gaseous H_2SO_4 concentration of $<2 \times 10^8$ cm^{-3} could be obtained with SIOMAS. Any H_2SO_4 vapor initially formed experiences rapid gas-to-particle conversion at plume ages <1.6 s, as expected from model results [*Kärcher et al.*, 1995].

3.5. Ultrafine Aerosols, Ions, and Sulfuric Acid Detected During SULFUR 5

[29] Shortly after S4, NASA colleagues performed similar experiments during a series of measurements in the SUCCESS project in April–May 1996 [*Toon and Miake-Lye*, 1998]. Moreover, first results were reported from the SNIF missions performed behind various jet aircraft (MD80, B727, B737, B747, B757, DC8, T-38) in January–May 1996 [*Anderson et al.*, 1998a, 1998b; *Cofer et al.*, 1998]. A strong increase of the number of volatile particles with FSC was found in the young plume [*Miake-Lye et al.*, 1998]. In the first preliminary presentation of the results of these measurements during a Conference at Virginia Beach in April 1996 it was suggested that the conversion fraction could reach up to 70%. Later publications on these experiments concluded ε values of 8 to 15% [*Anderson et al.*, 1998b], 31% (based on CIMS measurements of SO_2, analyzed FSC of the fuel used, and in situ CO_2 measurements) [*Miake-Lye et al.*, 1998], 26% [*Hagen et al.*, 1998], and 37% [*Pueschel et al.*, 1998]. The CIMS measurements during SUCCESS behind a B757 indicated that the conversion fraction increases from 6% for low FSC (72 μg/g) to 31% for high FSC (676 μg/g). In discussing the differences, it was argued that the S2 measurements might possibly underestimate the fraction of ultrafine particles [*Anderson et al.*, 1998b]. Therefore we performed a further experiment with enhanced capability to measure volatile and also nonvolatile fractions of ultrafine particles, and sulfuric acid in the gas phase and in the liquid particle phase, see below.

[30] Compared to S4, the fine mode aerosol sampling system (CPCs with $d > 5$ and 14 nm) was principally modified by a passive sample dilution to increase the detectable particle concentration range to about 5×10^5 cm^{-3} [*Schröder*, 2000]. A heating section was introduced to (alternatively) evaporate the volatile aerosol fraction for exclusive detection of the soot particle number density. Further, an infrared CO_2 sensor, a frost point hygrometer, two different mass spectrometer instruments, and canisters for air grab sampling were added to the Falcon payload, see Table 2.

[31] The Falcon chased the ATTAS at two altitudes and at distances between 70 and 3100 m. Fuels with low and high FSC (22 ± 2 and 2700 ± 350 μg/g) were used at conditions with and without contrail formation, see Table 4.

[32] Aerosol measurements were presented by *Schröder et al.* [1998]. Soot emissions were found to show no significant dependence on FSC. Evidence was given that at least 1/3 of the soot particles was lost from the interstitial aerosol. Thus soot has been involved in the ice nucleation process, possibly in addition to freezing of newly formed volatile particles. For the ultrafine ($d = 5 - 14$ nm) volatile aerosol a distinct increase of the apparent EIs within the first 10 s plume age was documented for the first time, illustrating the dynamic growth processes of freshly produced aerosol past exit. Further, the S5 measurements revealed differences between volatile particle formation within and outside contrail environment. In the absence of contrails the number of volatile particles with diameters >5 nm reaches 10^{17} kg^{-1} for high FSC and still reaches 10^{16} kg^{-1} for low FSC. In contrails, ultrafine particles were found diminished by significant fractions, most likely due to scavenging by ice crystals in the aging plume. A clear correlation between FSC and volatile particle growth was observed. The size spectra are bimodal with many volatile particles for large FSC in a diameter range near 14 nm.

[33] The observations provided important data to test models of aerosol formation in engine plumes. Model studies showed that the observed growth of ultrafine particles cannot be explained by classical homogeneous nucleation theory, but is reproduced in detail by a microphysical simulation when including CI emissions (sum of positive and negative ions) of 2.6×10^{17} per kg of fuel [*Kärcher et al.*, 1998b; *Yu et al.*, 1998]. The model explains the measured bimodal size spectrum with enhanced coagulation by charged particles [*Yu and Turco*, 1997]. The mode above 14 nm results from quickly growing charged particles, while only a few of the neutral particles grow to the detected size of >5 nm diameter. For high FSC the volatile material is consistent with a fuel sulfur to H_2SO_4 conversion fraction ε of 1.8%. For low FSC (22 μg/g) an unrealistically high conversion of 55% would be required to explain the volatile material measured. It was suggested that part of the volatile material results from condensable exhaust hydrocarbons. Further support for this conclusion was given in a follow-up study by *Yu et al.* [1999].

[34] Total sulfuric acid (gas plus aerosol) concentrations from engine exhaust was for the first time directly measured in the exhaust plume of a jet aircraft in flight with the Volatile Aerosols Component Analyzer (VACA) [*Curtius et al.*, 1998; *Curtius and Arnold*, 2001]. The instrument consists of a backward facing sample inlet, a heated flow tube (90°–120°C), an ion source injecting nitrate ions to chemically ionize sulfuric acid, and a quadrupole mass spectrometer to detect the ions. The heater evaporates the volatile components of small aerosol particles entering the instrument. The detection limit for H_2SO_4 concentration is 10^7 cm^{-3}. Owing to a number of loss processes, the obtained H_2SO_4 concentrations are regarded as lower-limit values. The measurements were verified during a first flight by injecting sulfuric acid directly into the exhaust jet at engine exit and measuring it in the aged plume. The mass spectra obtained in the exhaust of sulfur-poor fuel during the second S5 flight did not differ from the background spectra showing only the reactant ions NO_3^- $(HNO_3)_m$ with $m = 0$ and 1. However, for the sulfur-rich fuel the spectra show clear signatures of sulfuric acid: HSO_4^-, HSO_4^- (HNO_3), and HSO_4^- (H_2SO_4), at 97, 160, and 195 amu, respectively. The H_2SO_4 concentration reached values as high as 1500 pmol mol^{-1} (background: 10–50 pmol mol^{-1}) and was closely correlated with increases of temperature and CO_2 mixing ratio, see Figure 2. A conversion fraction

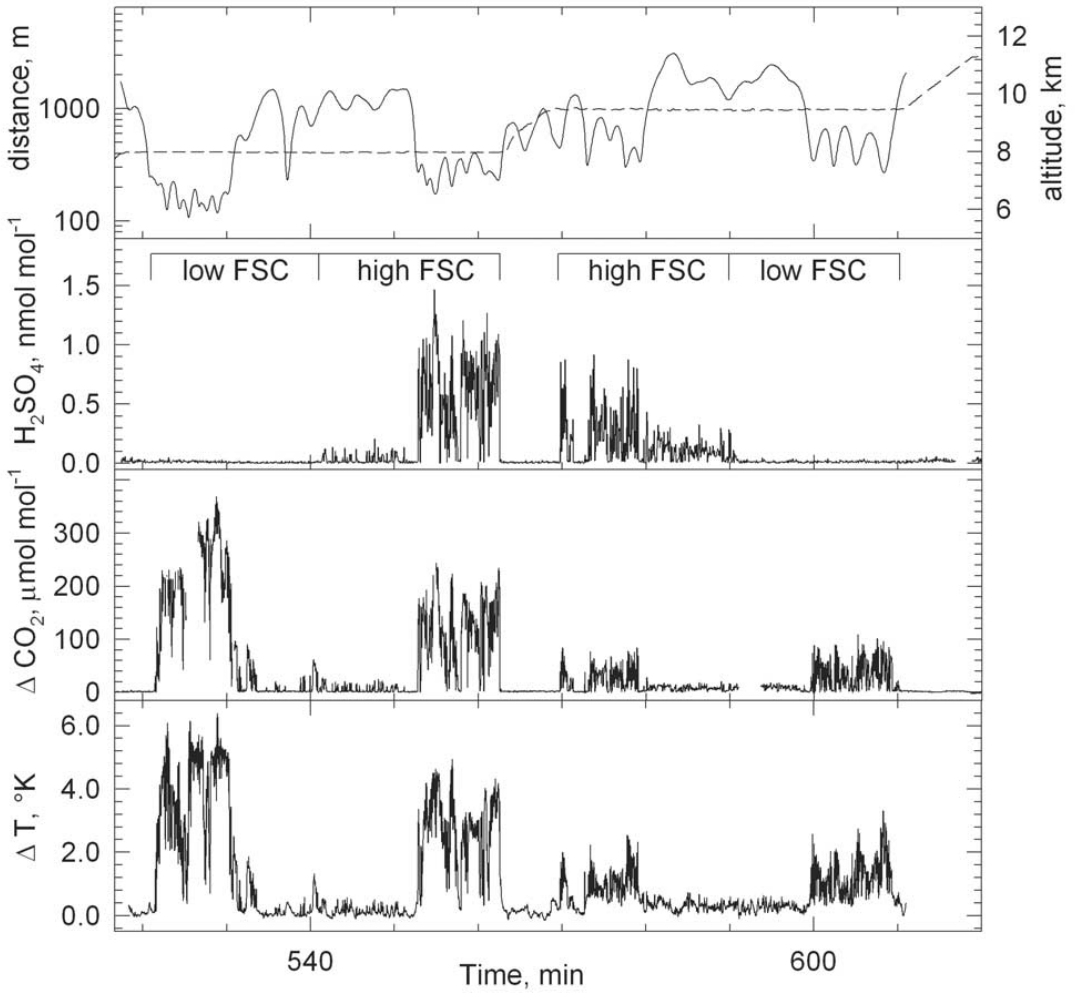

Figure 2. First measurements of sulfuric acid concentration and the conversion fraction ε of fuel sulfur into sulfuric acid in the engine exhaust gases of a jet aircraft at cruise during SULFUR 5 by VACA [*Curtius et al.*, 1998]. During flights of the Falcon at 8 to 10 km altitude, 70 to 300 m behind the ATTAS, clear increases in carbon dioxide ($\Delta CO_2 \approx 200$ µmol mol^{-1}) and temperature ($\Delta T \approx 3.5$ K) were measured in the exhaust plume. The temperature and CO_2 increases imply dilution factors N (amount of exhaust mass per unit mass of burned fuel) of $N \approx 10^4$ for the given example, which is consistent with the dilution law $N(t) = 7000\ (t/t_0)^{0.8}$, $t_0 = 1$ s, for a plume age t of 1.6 s [*Schumann et al.*, 1998]. When the ATTAS was burning fuels with high fuel sulfur content (FSC = 2700 µg/g), the measurements show clearly correlated increases in sulfuric acid ($\Delta H_2SO_4 \approx 1$ nmol mol^{-1}). The ratio of signals implies $\varepsilon = (\Delta H_2SO_4/\Delta CO_2)\ (32/44)\ EI_{CO2}/FSC \approx 0.4\%$ (32/44 is the ratio of molar masses of S and CO_2). Because of potential wall losses within the instrument and the inlet, this value represents a lower bound to the actual conversion fraction. No increase in ΔH_2SO_4 was detectable when the ATTAS engines were burning fuel with low FSC (22 ± 5 µg/g). Taking into account background fluctuations and statistical scatter, the conversion fraction at low FSC cannot be larger than 2.5 times the value at high FSC.

of fuel sulfur to H_2SO_4 of at least 0.34% was deduced from these data [*Curtius et al.*, 1998].

[35] If the conversion fraction would be the same for the low as for the high FSC, the expected increase is below 12 pmol mol^{-1} even for very young plume ages. During penetrations of the sulfur-poor plume the sulfuric acid concentration did not increase significantly above the local atmospheric background level of 15 to 50 pmol mol^{-1}. A

signal should have been visible if the conversion fraction at low FSC would be 2.5 times larger than at high FSC. Hence the conversion rate at low FSC was <2.5 the value at high FSC [*Curtius et al.*, 1998]. If the upper bound for ε is 1.8% at high FSC, as inferred from matching the measured aerosol number concentrations with $d > 5$ nm and $d > 14$ nm with aerosol models including CIs [*Yu and Turco*, 1998a; *Kärcher et al.*, 1998b; *Yu et al.*, 1998], an upper bound at low FSC for the ATTAS is 4.5%. This value is not far off the value 6% computed by *Brown et al.* [1996b] for the ATTAS engines at low FSC.

[36] In the first S5 flight a further instrument (Large Ion-Mass Spectrometer, LIOMAS) was flown on the Falcon to measure gaseous negative ions in the exhaust plume of the ATTAS jet aircraft in flight [*Arnold et al.*, 1999]. It was found that by far most of the negative ions had mass numbers >450 amu and number densities which markedly exceeded the number densities of ambient atmospheric ions. The large concentrations measured suggest that the massive ions observed inside the plume originated from CIs in the jet engines. The results for the low FSC suggest that the massive ions consist at least partly of species other than sulfuric acid. The measured number density of ions decreased faster than expected from dilution. A total negative ion concentration of $>5 \times 10^4$ cm^{-3} for a plume age of 1 s was inferred. The measured data represent lower bounds due to partial losses of the ions on the walls of the sampling tubes, and from the growth of charged particles beyond the size detectable by the instrument [*Arnold et al.*, 1999; *Wohlfrom et al.*, 2000].

3.6. Ultrafine Particle and Ion Composition and Size Distribution During SULFUR 6

[37] The previous measurements provided much progress in identifying the number of ultrafine particles, but the size spectrum of particles was still poorly defined because of missing continuity from the smallest clusters to the particles which can be measured optically at sizes of ~100 nm and larger. Moreover, first measurements with a new LIOMAS instrument revealed surprisingly large ions in the exhaust plume of the DC8 (0.5 to 1.5 s plume age) during the POLINAT 2 experiment. Gaseous H_2SO_4 was additionally detected by SIOMAS in the exhaust plume of the DC8 (about 3×10^9 cm^{-3} at 1 s plume age), possibly because of the smaller plume age compared to the A310 case (details to be described elsewhere).

[38] Therefore S6 was performed. The measuring concept remained basically unchanged compared to S5. However, the alternatively operating heating section of the CPCs ($d >$ 14 nm) was replaced by a parallel monitoring of the non-volatile aerosol fraction with $d > 10$ nm and great effort was spent to achieve a more detailed size resolution for nuclei and Aitken mode aerosols. Furthermore, a soot photometer and a nephelometer were integrated for an independent determination of the aerosol absorption and scattering coefficients. The FSSP-300 was modified for the detection of ice crystal concentrations larger than 5000 cm^{-3} by additional monitoring of the probe's electronic "activity" to determine and correct for the actual dead time fraction during the measurement [*Schröder et al.*, 2000a]. For the first time the particle size distributions from 3 to 60 nm diameter were determined using an extended set of 10 CPCs operated in parallel with successively increasing lower size detection limits (Table 2). By normalization with simultaneously measured CO_2 concentrations an apparent particle emission index (PEI) was determined [*Brock et al.*, 2000; *Schröder et al.*, 2000b]. Moreover, an improved LIOMAS instrument with increased mass range (1–8500 amu) [*Wohlfrom et al.*, 2000] and an improved VACA instrument were provided with reduced surfaces in the internal heating system reducing possible wall losses, and the instrument was calibrated with sulfuric acid/water aerosol particles in the laboratory [*Curtius and Arnold*, 2001].

[39] In situ measurements were performed at cruise altitudes behind the ATTAS and a B737 aircraft. Measurements were made 0.15–20 s after emissions as the source aircraft burned fuel with various FSCs, see Table 4. Measurements of ultrafine aerosol particles showed that nonsoot particles were present in high concentrations [*Schröder et al.*, 2000b; *Brock et al.*, 2000]. The actually detected numbers of particles formed correspond to particle EIs exceeding 1×10^{17} kg^{-1} and 2×10^{16} kg^{-1} for particles >3 nm and >5 nm, respectively. Consequently, the true concentrations of volatile aerosols (including the fraction below 3 nm) were estimated to exceed 2×10^{17} kg^{-1}. Volatile particle emissions did not change significantly with FSC when FSC was reduced below 100 μg/g. The measured particle emissions increase with plume age. The particle number concentrations are much smaller (by about a factor 4–8) in plumes at ambient conditions where contrails form than in plumes without contrails. The experiments give again clear indications that nonsulfate compounds, most likely condensable hydrocarbons, begin to dominate the volatile particle composition as FSC decreases below about 100 μg/g. The EI for volatile particles is only weakly dependent on the engine type.

[40] In addition to the results of S4 and S5, S6 was used to determine the emissions of soot (nonvolatile particles) from the ATTAS, the A310, and the B737 [*Petzold et al.*, 1999]. Soot number densities varied from 3.5×10^{14} (B737) to 1.7×10^{15} kg^{-1} (ATTAS), with corresponding mass EIs of 0.011 g kg^{-1} to 0.1 g kg^{-1}. The combination of soot photometer and integrating nephelometer showed an aerosol single-scattering albedo of about 1 outside the plume and <0.01 inside the plume which clearly indicated that by far the largest fraction of emitted particles is composed of black carbon. Additionally, the soot photometer for the first time provided a direct in-flight measurement of the emitted soot mass which agreed very well with soot mass concentrations calculated from measured size distributions [*Petzold et al.*, 1999].

[41] A new correlation method was set up to estimate the mass EIs based on available ground measurements. The measured and computed values agree within about 10% at cruise conditions. The correlation method was used to estimate the mean EI of soot by the globally operating aircraft fleet of 1992 to be 0.038 g kg^{-1} [*Petzold et al.*, 1999].

[42] Ice crystal concentrations inside young contrails were measured with the improved FSSP-300 to reach 4×10^4 cm^{-3} and $8–10 \times 10^4$ cm^{-3} for the B737 (plume age 0.4 s, FSC = 2.6 μg/g) and the ATTAS (1 and 20 s, 2.6 and 118 μg/g). The results were confirmed by extrapolation of measurements carried out at larger distances and correspond

to PEIs of 3.6 × and 15 × 10^{14} kg^{-1} with about 50% uncertainty.

[43] Total sulfuric acid concentrations were measured behind the B737 with the mass spectrometer instrument VACA in the very young plume (>0.15 s). Unfortunately, the upper FSC values of the fuels provided at Munich airport (56 μg/g) were rather small. Sulfuric acid (up to 8 × 10^9 cm^{-3} or about 600 pmol mol^{-1}) produced from fuel sulfur was detected when the engines burned fuel with FSC = 56 μg/g, but for the extremely low FSC = 2.6 μg/g a slightly enhanced (with respect to the background) H_2SO_4 concentration was registered only at the shortest distance. From the simultaneous CO_2 and H_2SO_4 measurements a conversion fraction of fuel sulfur to H_2SO_4 of ε = 3.3 ± 1.8% was deduced for the case of FSC = 56 μg/g [*Curtius et al.*, 2002]. The ε value is larger than the lower limit ε of 0.34% for the ATTAS, possibly because of the different engine (see below). However, the larger value also results because of reduced and calibration-corrected inlet wall losses. This is the first absolute and direct measurement of the conversion fraction of fuel sulfur in the exhaust plume of an aircraft. The direct method is considered to give results which are more reliable than those derived indirectly from aerosol data.

[44] For comparison, if the volatile aerosol contains only H_2SO_4 and H_2O, *Brock et al.* [2000] derived 2.4 ± 0.8% conversion from the aerosol size distribution in the diameter range 3 to 10 nm at plume ages 0.4 to 0.6 s. On the basis of observed growth of particles with plume age they expected 2–3 times larger values in the mature plume. An analysis of the CPC data with the model by *Kärcher et al.* [2000] (described below) suggests even larger (factor 10) increases in aerosol volume by 3 s plume age, so that this cannot be used to derive a realistic upper limit for ε.

[45] Both negative and positive CIs were measured by LIOMAS in flight in the plume of the ATTAS at plume ages of 0.6 and 6.2 s [*Wohlfrom et al.*, 2000]. Massive ions were detected with a quadrupole mass spectrometer of high sensitivity and low mass discrimination. It is operated in an integral high-pass mode where all ions above a lower cutoff mass pass the quadrupole rod system and are detected by a channel electron multiplier; scanning the cutoff mass results in an integral mass spectrum. CI mass distributions were obtained for mass numbers up to 8500 amu, and additionally the total number of CIs exceeding this size limit was determined.

[46] Both positive and negative CIs were found to be very massive even when nearly sulfur-free fuel was burned in the ATTAS engines (FSC of 2 μg/g). Observed positive CIs have a smaller mean mass compared to negative CIs. The raw CI data are CI counts in arbitrary units. The data were normalized to fit the size spectra derived from the CPC counters, see Figure 3. The normalized CI data extend the particle size spectra into the range below 3 nm, the presently lowest detectable particle size for CPCs. The spectral shape of the particle distributions measured by CPCs [*Schröder et al.*, 2000b] and detected by the IOMAS [*Wohlfrom et al.*, 2000] for the first time resolve the main mode position close to 3 nm diameter. The positive CI concentrations have a maximum near d = 1.5 nm. The size distribution of positive ions was similar for two FSC values (2 and 118 μg/g), while the size distribution of the negative CIs was shifted toward larger sizes. For FSC = 118 μg/g a significant number of the ion population seems to be larger than 2.8 nm [*Wohlfrom et al.*, 2000]. Similar behavior was modeled in detailed numerical simulations [*Yu et al.*, 1999]. In ground-based measurements, no significant CI-growth was observed when the FSC was raised from 2 to 66 μg/g [*Kiendler et al.*, 2001]. Hence, whereas the positive CIs do not grow strongly from sulfur but more likely from low volatility hydrocarbons, the negative CIs do grow with increasing FSC. CIs are present also in the size range measured with CPCs.

[47] Composition measurements of negative and positive CIs were made by a novel quadrupole ion trap mass spectrometer. Measurements were taken behind the ATTAS and other jet engines at ground and over a kerosene burner flame in the laboratory by *Kiendler et al.* [2000a, 2000b]. Unambiguous mass determination and identification of the chemical nature of ions were performed. The measurements indicate that sulfuric acid does not tend to strongly condense on positive ions and that positive ions in aircraft jet engine exhaust contain preferably organic molecules [*Kiendler et al.*, 2000b]. This is consistent with model assumptions [*Yu et al.*, 1999].

[48] Total positive CI concentrations in the ATTAS engine exhaust at the ground were measured [*Arnold et al.*, 2000] using an electrostatic probe (Gerdien-condenser). For a plume age of 12 ms, 1.4 m behind the engine exit, the positive ion concentration was 1.6 × 10^8 cm^{-3}. The number of positive ions decreases rapidly with increasing plume age, but is independent of FSC. When both ion-ion recombination and plume dilution are taken into account, it seems that the initial ion concentration at the engine exit plane is about 1 × 10^9 cm^{-3}, corresponding to a CI number EI of about 10^{17} kg^{-1} [*Arnold et al.*, 2000]. A more detailed model analysis by *Sorokin and Mirabel* [2001] finds for the same data a maximum concentration for the positive and negative ions at engine exit at ground of 0.8 × 10^9 cm^{-3} with an uncertainty of ±30%, which is not essentially different from the above 1 × 10^9 cm^{-3}. One should note that the ion concentration is likely to be much larger at combustor exit than at engine exit [*Starik et al.*, 2002].

3.7. Engine Technology Influence on Contrails and Particles in SULFUR 7

[49] The most recent S7 experiment was performed to test the influence of engine efficiency on contrail formation. Such an influence was expected based on S1 and in the meantime deduced from many individual contrail observations during POLINAT and SUCCESS [*Jensen et al.*, 1998a; *Kärcher et al.*, 1998a; *Schumann*, 2000], but direct evidence for different contrail formation from two aircraft with different engine efficiencies was missing. In the experiment, contrail formation was observed behind two four-engine jet aircraft with different engines flying wing by wing. The two contrail forming aircraft were a Boeing B707 and an Airbus A340. The two aircraft were selected for this test because the modern A340 engines provide significantly higher engine efficiency than those of the older B707 with lower bypass and pressure ratio, see Table 3. An altitude range exists, see Figure 1d, in which the aircraft with high engine efficiency causes contrails, while the other aircraft with lower engine efficiency causes none [*Schumann et al.*,

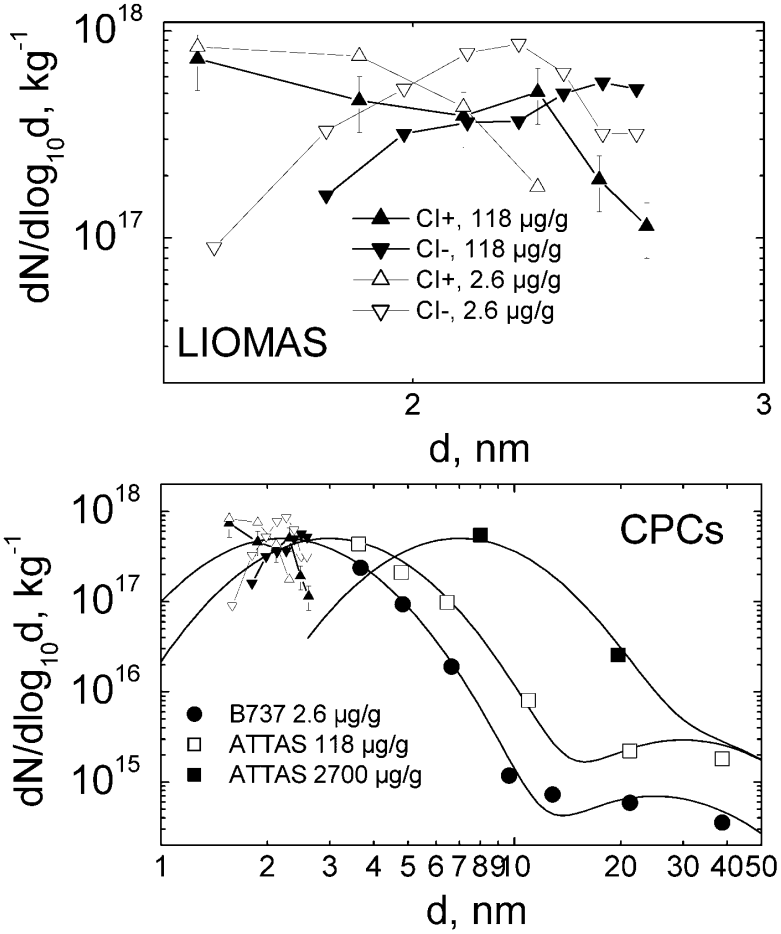

Figure 3. Number size distributions of CIs per unit mass of fuel burned (top and bottom panel) as obtained with LIOMAS behind the ATTAS during SULFUR 6 [*Wohlfrom et al.*, 2000] and plume aerosol particles (bottom panel) measured with CPCs during SULFUR 5 and 6 [*Schröder et al.*, 2000b] for different FSCs. The three bimodal distributions (bottom panel) represent parameterizations of measurements behind the B737 (2.6 μg/g FSC) and the ATTAS (118 and 2700 μg/g FSC). The CI data are for 2.6 and 118 μg/g FSC (open and solid symbols) for positive (triangle upward) and negative ions (triangle downward). The mass bins of the spectrometric measurements were converted to particle diameters assuming spherical particles with density 1.4 g cm^{-3}. It should be noted that the LIOMAS does not detect any neutral particles which may have been formed via recombination of positive and negative ions in the very young exhaust plume, and provides normalized spectra only. Therefore the LIOMAS data have been normalized to fit the aerosol data assuming a total number of particles (CIs of either sign and CNs) corresponding to a particle emission index of 2.0 and 2.4 $\times$ 10^{17} kg^{-1} for 2.6 and 118 μg/g FSC, respectively.

2000b]. Table 4 shows that all contrails were observed in close accordance with the Schmidt/Appleman criterion.

[50] The aerosol measurements in the young plumes of the A340 (Table 4, near flight level 314) and B707 (310) with typical FSC values (380 and 120 μg/g) and at non-contrail-forming conditions, at close separation (70 to 140 m; determined from photos, see Figure 1f) reveal strong differences, see Figure 4. The number of nonvolatile (mainly soot) particle emissions is about 1 order of magnitude larger for the B707 than for the A340, see Table 6. The data in this table are based on events with peak plume concentrations (12–15 in number) inside the young plume, with typically ±30% uncertainty. The volume size spectrum of the B707 is dominated by particles measured with the

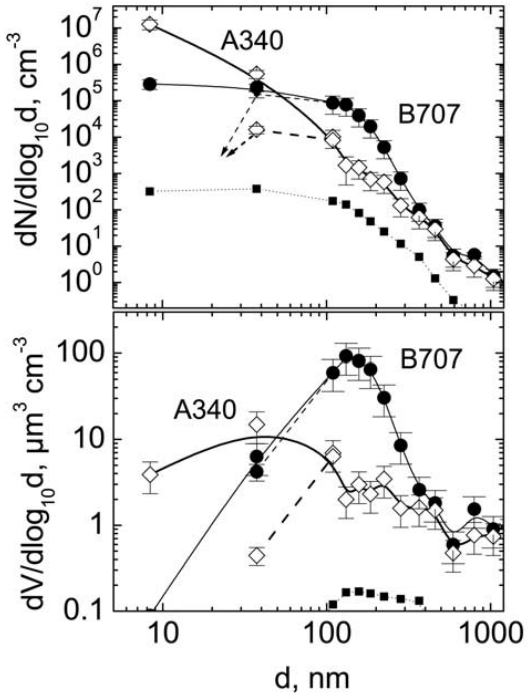

Figure 4. Number density data of total aerosol interpolated with straight lines (top) and volume density data of nonvolatile aerosol fitted by bimodal long-normal distributions (bottom) versus particle diameter d of jet exhaust aerosol under noncontrail-forming conditions for the B707 (solid curves, solid circles) and the A340 (dashed curves, open circles) aircraft during SULFUR 7, and in the background atmosphere (dotted curve, solid diamonds). For $d > 100$ nm the results are from the PCASP wing station (assuming refraction indices of black carbon for the plume aerosol and polystyrene latex spheres for the background aerosol). The data at 8 nm (5–14 nm range) and near 16 to 30 nm (14–110 nm range) are based on CPC measurements without heating (top) or after heating to 500 K (bottom). Note that for $d < 100$ nm, S7 provided far less size resolution than S6.

PCASP. The optical properties of the particles and the volume spectra are derived assuming spherical soot particles which may be debatable. The soot mass EIs determined from these data, see Table 7, show a trend toward less soot emissions with more modern engine technology. The number of volatile particle emissions detected with diameter >5 nm (the majority concentrated in the nuclei mode range) differed even more and in the opposite way, see Figure 4 and Table 6. The surface and volume densities differ also strongly, see Table 6. The available aerosol surface area in the young, noncontrail plume is bound to the lower accumulation mode range around 100 nm diameter for the B707 case but widely shifted into the Aitken mode (~50 nm) for the A340-case. The PEI for the A340 are about 10 times larger than for the B707, see Table 8. The differences in the engines go along with differences in the EIs for CO which we measured during these flights: A340, 1.9 g kg^{-1}; B707, 14.4 g kg^{-1}. While the old engines emit more aerosols by mass, the modern engines contribute a larger number of (ultrafine) particles.

[51] If one would assume that the volatile material is composed of sulfuric acid and water only, a volume density v of volatile aerosol (Table 6) would imply a conversion fraction $\varepsilon^* = \rho_{acid} v\, x_{acid}\, N\, 32/(98\ \mathrm{FSC}\ \rho)$, with acid density ρ_{acid} = 1.8 g cm^{-3}, acid mass fraction x_{acid} = 0.92, air density ρ, and dilution factor N = 5000. This yields ε^* = 1.6, 22, and 25% for the A340 and 0.4, 21, and >100% for the B707, depending on whether one computes the volume just from the numbers of volatile particles counted with the CPCs and their cutoff diameters of 5 and 14 nm, or takes the values derived from the volume distribution as listed in Table 6 without or with the volume measured with the PCASP. The maximum values are clearly unrealistic. These considerations show the large uncertainty range of such estimates.

[52] The in-flight measurements in the wakes of the A340 and B707 aircraft with the LIOMAS instrument confirmed that already 70 to 140 m behind the engine, 50–60% of the negative CIs formed during combustion have grown to masses of more than 8500 amu, in particular for the A340.

4. Discussion

4.1. Fuel Sulfur to Sulfuric Acid Conversion Fraction

[53] Conversion fractions ε (per molecule) derived from the SULFUR experiments, as well as from SUCCESS

Table 6. Aerosol Concentrations in the Young Plume Behind the A340 and B707 Aircraft During S7, and in the Background Upper Troposphere

Aerosol Data[a]	Unit	A340	B707	Background
		Total Aerosols		
Number $d > 5$ nm	cm^{-3}	4×10^6	3×10^5	500
Number $d > 14$ nm	cm^{-3}	5×10^5	2×10^5	420
Surface	µm^2 cm^{-3}	3000 (70)	1900 (1100)	5
Volume	µm^3 cm^{-3}	15 (2)	32(28)	0.2
		Nonvolatile Particles		
Number $d > 10$ nm	cm^{-3}	0.15×10^5	1.5×10^5	<50

[a]Concentrations per unit volume; numbers in parentheses denote the contributions from particles measured with the PCASP; estimated plume age 0.4 to 0.8 s; concentrations are given for plume conditions with dilution factor 5000, based on temperature and humidity increases measured in the plume. The uncertainty is typically ±30%. The total number concentration of particles with $d > 5$ nm behind the A340 may reach as high as 10^7 cm^{-3} because the CPC counter of type TSI 3760A used was close to saturation (coincidence correction included).

Table 7. Soot Mass and Number Emission Indices at Cruise and Smoke Numbers[a]

Aircraft	EI_{soot}, g kg^{-1}	PEI_{soot}, 10^{15} kg^{-1}	SN at 100%	SN at 30%
B707	0.5 ± 0.1	1.7 ± 0.3	54.5	n.a.
ATTAS	0.1 ± 0.02	1.7 ± 0.35	46.3	10.9
A310	0.019 ± 0.01	0.6 ± 0.12	5.8	n.a.
B737	0.011 ± 0.005	0.35 ± 0.07	4	2.5
B747		0.27, 0.45	16.0	n.a.
DC10		0.46	11.4	1.6
A340	0.01 ± 0.003	0.18 ± 0.05	12.6	1.0

[a]EI_{soot} and PEI_{soot}: soot mass and number emission indices per unit mass of fuel burned; smoke number (SN) at two power settings from *ICAO* [1995] as far as available; data for ATTAS, A310, and B737 from *Petzold et al.* [1999]; for B747 and DC10 from measurements performed by the University of Missouri-Rolla [*Schumann et al.*, 2000a]; B707 and A340 from this work. EI_{soot} values are derived by fitting bimodal lognormal distributions to the PCASP and the nonvolatile CPC data, see Figure 4 [*Petzold et al.*, 1999].

(measurements behind a B757 [*Miake-Lye et al.*, 1998]), the Concorde [*Fahey et al.*, 1995], from the Lufthansa ground test facility [*Frenzel and Arnold*, 1994], and from POLINAT 2 [*Schumann et al.*, 2000a] are compiled in Table 8. The table collects the data for different lower cutoff sizes of the particle counters, plume ages from 0.15 to 3360 s, FSC values from 2.6 to 5500 μg/g, different instrument techniques, different methods to indirectly derive ε values, and various aircraft/engine combinations at cruise or at ground. The table extends a similar one of *Brock et al.* [2000].

[54] The only direct measurements of sulfuric acid in the exhaust plume of cruising aircraft are those obtained for the ATTAS and B737 aircraft. The measurements behind the ATTAS reveal a conversion of fuel sulfur to sulfuric acid with fraction $\varepsilon > 0.34\%$ [*Curtius et al.*, 1998], consistent with direct measurements at ground during S3 ($\varepsilon = 1.2\%$, at FSC of 212 μg/g) [*Arnold et al.*, 1998a], and in accordance with the early result ($\varepsilon > 0.4\%$) measured at ground by *Frenzel and Arnold* [1994]. The amount of volatile material found at high FSC suggests $\varepsilon < 1.8\%$ [*Yu and Turco*, 1998a; *Kärcher et al.*, 1998b; *Yu et al.*, 1998], and the combined VACA/CPC findings imply $\varepsilon < 4.5\%$ at low FSC for the ATTAS. For the B737, ε is measured to be 3.3 ± 1.8% for the rather low FSC of 56 μg/g [*Curtius et al.*, 2002].

[55] Otherwise, the listed apparent ε values (denoted by ε*) are derived from volatile particle volume measurements in the young exhaust plume for various FSC values. For low FSC values some of the results imply $\varepsilon^* > 50\%$. The low-sulfur aerosol data measured behind the ATTAS would imply even larger ε* fractions than derived elsewhere, and the results for the B707 and A340 are within the same range as the SUCCESS results [*Toon and Miake-Lye*, 1998]. Such large conversion efficiencies cannot be explained by sulfuric acid formation with model computations for reasonable engine emissions [*Brown et al.*, 1996b; *Lukachko et al.*, 1998; *Tremmel and Schumann*, 1999; *Miake-Lye et al.*, 2001; *Starik et al.*, 2002], nor are they consistent with measurements at the ground [*Arnold et al.*, 1998a; *Hunton et al.*, 2000]. The aerosol-derived ε* depends strongly on the cutoff diameter d above which more than 50% of the particles are counted; on possibly an enhanced counting efficiency for charged clusters; on the width of the detector size sensitivity, in particular for small d; on the shape of the aerosol number spectrum which folds with the detector sensitivity function; on wall losses of small or very large particles in the inlet [*Cofer et al.*, 1998], possibly with enhanced wall losses for charged particles; and on enrichment effects due to nonisokinetic sampling of ice particle residuals. A 21% uncertainty in d, which may be expected [*Wilson et al.*, 1983; *Brock et al.*, 2000; *Schröder et al.*, 2000b], implies 50% uncertainty in ε*. Variations in the particle counter sensitivity and aerosol spectrum may cause up to 50% uncertainty in ε* for $d < 10$ nm if not carefully corrected [*Brock et al.*, 2000]. The detection sensitivity of a CPC to charged molecule clusters is unknown [*Yu and Turco*, 1998b]. A large enrichment of residuals from ice crystals larger than about 1 μm cannot be excluded if forward looking aerosol inlets are used [*Konopka et al.*, 1997]. For the same reason, the interstitial aerosol inlet does not count the volatile aerosol contained in contrail ice particles [*Schröder et al.*, 2000b]. *Brock et al.* [2000] concluded a relative uncertainty of ±38% for the ε* values derived for the B737 at FSC = 56 μg/g, including uncertainties in FSC. Otherwise, it must be assumed that much of the scatter in the reported ε* values is due to uncertainties mainly with respect to particle composition.

[56] The strong increase in the aerosol derived ε* for small FSC values indicates that condensable gases other than sulfuric acid contribute to the formation of volatile particles in the young exhaust plume, as originally suggested by us during the panel discussion at the International Colloquium "Impact of Aircraft Emissions Upon the Atmosphere," Office National d'Etudes et de Recherches Aérospatial (ONERA), Chatillon, Paris, 15–18 October 1996. The conjecture was introduced to offer an explanation for the large fuel sulfur conversion fraction ε reported by *Fahey et al.* [1995] from the Concorde measurements. These measurements could be explained only under the assumption that a large fraction of the fuel sulfur (25 to 60%) is converted to S^{VI} ($H_2SO_4 + SO_3$), already before leaving the engine exit [*Danilin et al.*, 1997; *Kärcher and Fahey*, 1997; *Yu and Turco*, 1998b]. Alternative explanations in terms of CIs [*Yu and Turco*, 1997, 1998b] or oxidation to S^{VI} in the plume by some "unknown" chemistry [*Danilin et al.*, 1997] could not explain the large amount of volatile material found behind the Concorde and in young exhaust plumes. In view of measured OH concentrations formed in the plume mainly by photolysis of nitrous acid [*Hanisco et al.*, 1997] and new laboratory studies, major sulfur oxidation in the aging plume can be excluded [*Rattigan et al.*, 2000]. An effort performed by *Konopka et al.* [1997] to deduce the sulfuric acid content in volatile particles from the measured particle size spectra

Table 8. Conversion Fraction of Fuel Sulfur to Sulfuric Acid and Particle Number Emission Indices From Various Studies[a]

FSC, $\mu g\ g^{-1}$	Aircraft	Engine	Experiment, Conditions	Technique	Plume Age, s	ε, %	d, nm	PEI_{soot}, 10^{15} kg^{-1}	PEI_{total}, 10^{15} kg^{-1}	Reference
2.6	B737	CFM56-3B1	S6, no contrail	CPC	0.2–0.6	>17 ± 6[b]	3	0.35	60	*Brock et al.* [2000], *Schröder et al.* [2000b]
	ATTAS	Mk501		CPC	0.5–7	>20–80[b]	4	1.8	100	*Schröder* [2000], *Schröder et al.* [2000b]
20	ATTAS	Mk501	S5, no contrail	CPC/model	0.8–10	>55[b]	5	1.7	5–20	*Kärcher et al.* [1998b], *Yu et al.* [1998]
				H_2SO_4-CIMS	>0.5	0.34 < ε <4.5[b]	...	...	...	*Curtius et al.* [1998], this work
56	B737	CFM56-3B1	S6, no contrail	CPC	0.2–0.6	>2.4 ± 0.8[b]	3	0.35	90	*Brock et al.* [2000], *Schröder et al.* [2000b]
				H_2SO_4-CIMS	>0.15	3.3 ± 1.8	...	...	...	*Curtius et al.* [2002]
72	B757	RB211	SUCCESS, contrail	CPC	0.2–80	8 ± 3[b]	4	0.2–0.9	1–2	*Miake-Lye et al.* [1998]
				SO_2-CIMS	0.2–80	6 (0–34)	...	...	...	*Miake-Lye et al.* [1998]
				CPC		8[b]	4	0.6 ± 0.1	1.4 (0.8–2)	*Anderson et al.* [1998b]
				DMA	10–100	19[b]	8	0.07[c]	0.28[c]	*Hagen et al.* [1998]
				impactor		37[b]	20	0.17[c]	...	*Pueschel et al.* [1998]
118	ATTAS	Mk501	S6, no contrail	CPC	>0.5	2.3[b]	3	1.8	150	*Schröder et al.* [2000b]
120	B707	JT3D-3B	S7, no contrail	CPC	0.4–0.7	(0.4–21)[b]	5	1.7	6	this work
170	ATTAS	Mk501	S2, contrail	CPC/model	20	(0.4–1.8)[b]	7		8	*Schumann et al.* [1996], *Yu and Turco* [1998a]
212	ATTAS	Mk501	S3, ground	CIMS (IOMAS)	0.0066	1.2	...		...	*Arnold et al.* [1998a]
230	Concorde	Olympus 593	Mach 2, no contrail	CPC	780–3360	>12,[b] >46[b]	9	43–87	17–650	*Fahey et al.* [1995]
				impactor	1107–1708	...	50	0.008[c]		*Pueschel et al.* [1997]
240	B747		POLINAT	DMA	84–90	0.4–21.7[b]	12	0.54	3.5	*Konopka et al.* [1997]
260	B747		POLINAT	DMA	119	1.1–40.7[b]	12	0.46	8.4	*Konopka et al.* [1997]
265	DC10		POLINAT	DMA	76–88	0.9–36.8[b]	12	0.27	10.1	*Konopka et al.* [1997]
380	A340	CFM56-5C4	S7, no contrail	CPC	0.5–0.8	(1.6–22)[b]	5	0.18	48 (32–100)	this work
480	A340	CFM 56-2C1	POLINAT 2, contrail	CPC	100	...	5	1.6	19–23	*Schumann et al.* [2000a]
676	B757	RB211	SUCCESS, contrail	CPC	0.2–80	>15 (±7)[b]	4	0.2–0.9	10–100	*Miake-Lye et al.* [1998]
				SO_2-CIMS	0.2–80	31 (15–52)	...			*Miake-Lye et al.* [1998]
				CPC		15[b]	4	0.5 ± 0.2	15 (4–40)	*Anderson et al.* [1998b]
				DMA	10–100	26[b]	8	0.28[c]	2.6 ± 0.4[c]	*Hagen et al.* [1998]
				impactor	33	10–26[b]	20	0.7–5.2[c]	...	*Pueschel et al.* [1998]
690	DC8	CFM 56-2-C1	POLINAT 2, contrail	DMA	1–5	...	7	0.011[c]		*Paladino et al.* [2000]
1000	...	modern engine	LH test site Hamburg	CIMS (IOMAS)	0.2	>0.4	...	...	...	*Frenzel and Arnold* [1994]
2700	ATTAS	Mk501	S5, no contrail	CPC	>0.5	1.8[b]	5	1.7	200	*Kärcher et al.* [1998b], *Yu et al.* [1998]
				H_2SO_4-CIMS	>0.5	0.34 < ε <1.8[b]	...	...	...	*Curtius et al.* [1998], this work
5500	ATTAS	Mk501	S2, contrail	CPC + models	20	(0.4–1.8)[b]	7	...	10	*Schumann et al.* [1996], *Yu and Turco* [1998a]

[a]The table is ordered by fuel sulfur content (FSC); ε = conversion mole fraction, d = cutoff diameter, PEI_{soot} and PEI_{total} = particle number emission indices of nonvolatile or "soot" particles and total (including volatile) particles per unit mass of fuel burned. Values in parentheses denote the possible range of results from the experiments.

[b]Calculated from particulate volume and presuming that the particles are exclusively composed of sulfuric acid and water, denoted by epsilon star in the text.

[c]The values derived from DMA and impactor instruments deviate from the CPC data, possibly because of inlet wall losses, other cutoff sizes, or smaller collection efficiency.

Table 9. Computed Engine Parameters and Conversion Fractions ε Compared to Measurements

Aircraft	Engine[a]	Flight Level, hft	Combustor Exit Teperature, K	Combustor Exit Pressure, hPa	Age at Engine Exit, ms	Temperature at Engine Exit, K	Pressure at Engine Exit, hPa	ε, %, Computed	ε, %, Measured
ATTAS	Mk501	310	1154	5243	5.2	581	288	3.4	0.4–4.5
ATTAS	Mk501	260	1154	5727	5.4	599	360	3.7	0.4–4.5
B737	CFM56	350	1237	6050	6.5	544	238	5.9	3.3 ± 1.8
B737	CFM56	260	1209	5987	7.5	592	360	5.6	3.3 ± 1.8
B747	RB 211	350	1540	11,000	4.6	598	220	9.6	...

[a]Cases ATTAS and B737 from G. Tremmel (personal communication, 1999); case B747 from *Starik et al.* [2002].

obtained during POLINAT indicated that even 100% conversion from fuel sulfur would not suffice to explain the measured volume of volatile material in exhaust aerosols in some cases, but oversampling of ice particles containing volatile particles could not be excluded. These discussions motivated studies to look for low volatility hydrocarbons, possibly including aldehydes, alkenes, and alkynes [*Kärcher et al.*, 1998b; *Yu et al.*, 1999]. Organic material was measured in soot by *Petzold and Schröder* [1998]. Evidence for the existence of organic material clusters in the exhaust is provided by "OHC ions" containing C and H atoms and in part also O atoms in negative CIs measured by *Kiendler et al.* [2000a].

[57] Engine chemistry models imply a decrease of ε with growing FSC because of the finite amount of oxidizing radicals available at the combustor exit. For the ATTAS engine, *Brown et al.* [1996b] computed ε = 6 % and 1% for FSC = 2 and 5400 μg/g, very close to the upper limits derived for ε in the present paper. Other studies [*Lukachko et al.*, 1998; *Tremmel and Schumann*, 1999; *Starik et al.*, 2002] deduced a weaker dependence on FSC. Most volatile aerosol data suggest a strong decrease of ε* with increasing FSC, but this may be misleading because of possible organic components. The increase in conversion fraction with FSC derived from SO_2, CO_2, and FSC data [*Miake-Lye et al.*, 1998] is likely an artifact due to problems in measuring the FSC, and the precision of the SO_2 and CO_2 data does not allow to determine the nonmeasured S^{VI} fraction as a remainder for conversion fraction values below 10 to 20% [*Hunton et al.*, 2000].

[58] The ATTAS ε* values of 55 and 1.8% for 20 and 2700 μg/g FSC could be unified with ε* of 1.4% and 40 μg/g emitted condensed organic material, but other ε* − FSC data pairs would imply different amounts of organic material ranging from 1 to 400 μg/g (with the maximum computed for the Concorde) for the same conversion fraction.

[59] The sulfur conversion fraction ε may depend on the engine and its state of operation. An engine chemistry model [*Tremmel and Schumann*, 1999] has been applied to compute ε for the thermodynamic conditions of the ATTAS and B737 engines during S5 and S6. The simulations (see Table 9) yield ε = 3.4–3.7% for the ATTAS engine and ε = 5.6–5.9% for the B737 (FSC = 100 μg/g in both cases). The computed values are within the range of measured values and show the same trend. The ε value is higher for the B737 engine than for the ATTAS because of the higher temperature and pressure behind the combustor. The model is applied with a prescribed exponential temperature and pressure decrease with time from combustor exit to engine exit fitted to engine data. With a different model and for another engine (RB211-524B, pressure ratio 28) with even higher combustor exit pressure and temperature, *Starik et al.* [2002], see Table 9, compute ε up to 10%, and confirm the increase of ε with combustor exit pressure and temperature. This is further supported by an analysis of S^{VI} formation as a function of pressure and temperature in an equilibrium model [*Miake-Lye et al.*, 2001]. The factor 6 to 18 larger number of volatile particles larger 5 nm measured behind the A340 compared to the B707 (see Tables 6 and 8) also strongly suggests that ε is larger for the engines of the A340 with high pressure ratio compared to those of the older B707. The parameters of the Concorde engines (Olympus 593 Mk610) [*Deidewig*, 1998] are between those of the B737 engine and the RB 211 (pressure ratio 10.6, combustor exit pressure and temperature 9000 hPa and 1430 K, no bypass, overall propulsion efficiency 0.4 at cruise with Mach 2, and maximum smoke number at ground without afterburner of 26.4). As noted before, some of the fast aircraft chased by the Falcon were operated at reduced power settings. Hence the possibility of larger values for certain engines and operation conditions, with higher combustion pressure, cannot be excluded from the measurements.

[60] A conversion of ε yields an equivalent H_2SO_4-emission index $\varepsilon \times FSC \times 98/32$, where 98/32 is the molecular weight ratio for H_2SO_4 and S. For ε = 3% and a typical FSC = 400 μg/g one obtains an equivalent $EI(H_2SO_4)$ of 0.04 g H_2SO_4 kg^{-1}. This is comparable to the mean EI_{soot} of 0.04 g kg^{-1}, but markedly exceeds the EI_{soot} of 0.01 g kg^{-1} of modern jet engines. If the mean diameter of the volatile particles is 5 nm, and their density is close to 1.5 g cm^{-3}, then 10^{17} such particles per kilogram correspond to a mass EI of 0.01 g kg^{-1}. The inferred EI of volatile material is smaller than the $EI(H_2SO_4)$. Hence, for typical FSC values, sulfuric acid remains the most important condensed material in the plume besides water.

4.2. Soot and Volatile Particles

[61] Additionally, Table 8 lists the particle number emission indices (PEI) of total (volatile and nonvolatile) and soot particles derived from the various measurements. From the SULFUR experiments, values $PEI = \Delta c\ N/\rho$ are derived from the measured particle concentrations Δc above background, air density ρ, and dilution factor N (mass of exhaust gases per unit mass of fuel burned), with N determined from measured tracers for fuel consumption (CO_2 concentration or temperature increase above ambient values; see Figure 2, for example), or from the observed plume diameter, or plume age and an empirical dilution law [*Schumann et al.*, 1998].

[62] The PEI for soot particles >50 nm identified in the Concorde plume with impactors [*Pueschel et al.*, 1997]

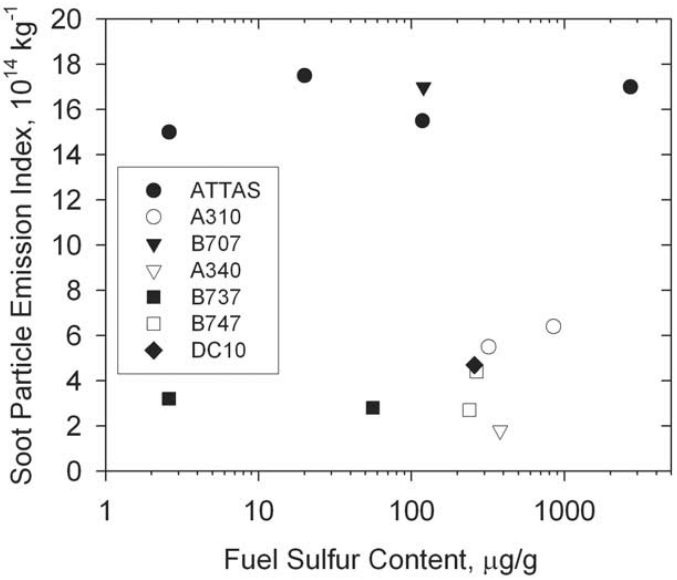

Figure 5. Soot particle number emission indices for particles >10 nm remaining after heating to 500 K versus fuel sulfur content. Data from S5, S6, S7, and POLINAT for various aircraft as listed. The ATTAS and B707 produce far more soot emissions than all other aircraft engines.

(computed from $EI_{soot} = \Delta c\ EI_{CO2} M_{air}/\{M_{CO2}\ \rho\ \Delta[CO_2]\}$ and the data from *Pueschel et al.* [1997]: $\Delta c = 0.21$ cm^{-3}, $EI_{CO2} = 3.16$, $M_{air} = 29$, $M_{CO2} = 44$, $\rho = 0.17$ kg m^{-3}, $\Delta[CO_2] = 0.34 \times 10^{-6}$) is 10^4 times smaller than the PEI of nonvolatile particles >9 nm counted with CPCs [*Fahey et al.*, 1995]; compatibility among both numbers and the reported soot mass emission index of 0.07 ± 0.05 g/kg [*Pueschel et al.*, 1997] would require a volume mean soot diameter <13 nm, which is not supported by other observations. The measurements obtained with CPCs behind several subsonic aircraft range from 2×10^{14} to 3×10^{15} kg^{-1}. Figure 5 shows that the soot EIs measured for the ATTAS and B737 do not depend on the FSC. The emissions vary mainly because of different engine technology, see Table 7, and show the same trend as the smoke number data of *ICAO* [1995] for lower than normal cruise power settings. The modern engines of the B737, B747, A310, A340, and DC10 have about a factor 10 smaller soot EIs than those of the older ATTAS and B707. For the particle size distribution of modern engines the aviation fleet of 1992 is estimated to emit 1.2×10^{15} kg^{-1} soot particles on average [*Petzold et al.*, 1999]. Slightly larger values measured in the North Atlantic flight corridor may include some volatile fractions [*Anderson et al.*, 1999a].

[63] For volatile particles the measurements generally show very large PEIs from less than 10^{15} to more than 10^{17} kg^{-1} increasing with decreasing cutoff diameter d and increasing FSC. Figure 6 summarizes the SULFUR results in noncontrail-forming plumes. The PEI for volatile particles larger than 5 nm increases by a factor of 10 for an increase of FSC from 2.6 to 2800 μg/g. Emissions of particles larger 14 nm increase by a factor of 5 over this range. Further data are available from the SNIF III experiments, showing a maximum PEI of 8.7×10^{17} kg^{-1} particles larger 4 nm when burning fuel in an afterburner (possibly enhancing CI formation) of an F-16 fighter aircraft [*Anderson et al.*, 1999b]. Part of the variation in the PEI values is due to different engines and flight conditions. The PEI value of the B707 is lower than that of the A340 possibly because of more soot and hence more scavenging of volatile aerosols. The ATTAS is in between these technologies. Ultrafine CN increases measured with different methods relative to nitrogen oxides increases in minutes to 10 hours old aircraft plumes revealed PEI values between 10^{16} and 1.2×10^{17} kg^{-1} [*Schlager et al.*, 1997; *Anderson et al.*, 1999a].

[64] The data cannot be explained by the classical theory of binary homogeneous nucleation of H_2SO_4 with H_2O. This theory implies PEI values for $d > 3$ nm which are far below the PEI results measured for FSC <1000 μg/g and grow steeper than linear with FSC, different from what is observed [*Kärcher et al.*, 2000]. The data can be explained only when taking ion-induced nucleation and ion-enhanced coagulation into account. For matching the data the models [*Yu et al.*, 1998; *Kärcher et al.*, 2000] require an initial total ion concentration at engine exit of 4×10^8 cm^{-3} at temperature $T = 600$ K and pressure $p = 220$ hPa, or an ion EI of 2×10^{17} CIs per kg of fuel burned. These assumptions are approximately consistent with the number of ions measured at ground with a Gerdien condenser [*Arnold et al.*, 2000]. The models do not include cluster growth inside the engine before reaching the exit. The details of formation, dynamics, and particle nucleation for

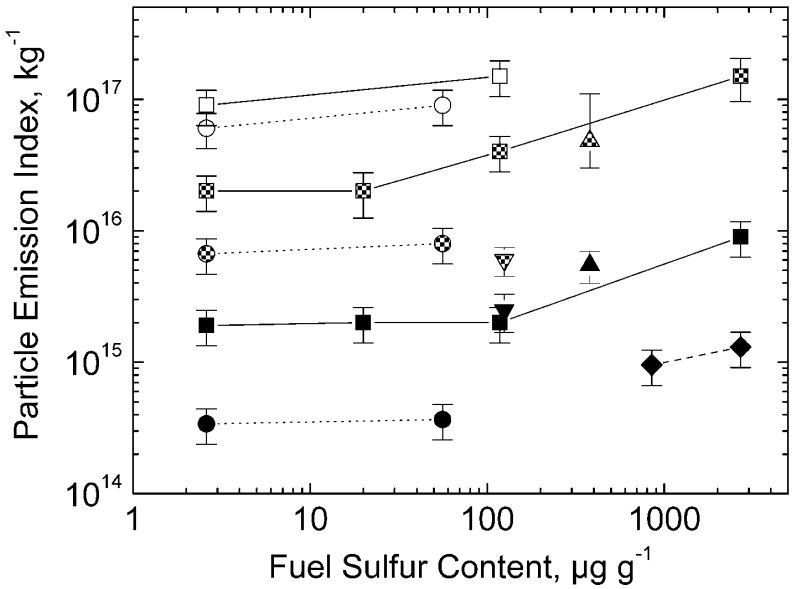

Figure 6. Emission index of the number of detectable volatile particles versus FSC in plumes without contrail formation, for various aircraft, lower detection limits d of particle diameters (open symbols: $d = 3$ nm; gray symbols: 5 nm; black symbols: 14 nm), and plume ages. ATTAS (squares) from S5, 7–9 s, and from S6, 0.5–7 s; B737 (circles) from S6, 0.4–0.6 s; A340 (upward pointing triangle) from S7, 0.5–1.5 s; and B707 (downward pointing triangle) from S7, 0.4–1.2 s. Note that the ATTAS values are higher than all others mainly because of the larger plume age.

ions, sulfuric acid, and condensable hydrocarbons from combustor exit to the nozzle exit have not yet been modeled.

[65] Much of the variation in volatile aerosols can be explained in terms of different size sensitivity of the CPC instruments, plume ages, and FSC values. *Kärcher et al.* [2000] provided an analytical model to explain the wide variance of observed PEIs in exhaust plumes. The model assumes that the number of CIs available determines the number of nanometer-sized volatile particles detectable with CPCs in the exhaust plume. The amount of sulfuric acid (depending on FSC and the conversion fraction ε) and the amount of condensable organic matter control the size of the particles formed. Coagulation and dilution control the timescales of particle growth. Using this model, and the parameters listed in Table 10, the measured PEIs can be normalized to a given plume age (3 s) and cutoff size of the particle counters (5 nm), see Figure 7.

Table 10. Parameters Used for Normalizing the PEI to Fixed Cutoff Size and Plume Age

Aircraft	Project	FSC, µg g^{-1}	EI_{OM}, µg g^{-1}	ε, %	EI_{CI}, 10^{17} kg^{-1}	d, nm	t, s	PEI,[a] 10^{17} kg^{-1}
Concorde		230	70	15	5	9	960–3480	1.4
ATTAS	S5, S6	2700, 118, 20, 2.6	20–35	3–6	1.5–2	3–5	2–8	1.5, 0.36, 0.096, 0.14
B737	SNIF-II	800	20	2	1.5	4	25	0.87
F16	SNIF-III	146, 527, 942	1	0.5–1	3–4	4	0.5–16	0.46, 0.38, 1.14
DC8	SUCCESS	550	10	1	1.5	4	20–40	0.51
B747	POLINAT	240, 265	10	2	2	12	84, 88	0.26, 0.28
DC10	POLINAT	265	18	2	2	12	120	0.22
B737	S6	2.6, 56	30	5	3	3	0.15–0.4	0.29, 0.45
A340	S7	380	20	5.5 (4–12)	1.1 (0.9–1.8)	5	0.7	1.8
B707	S7	120	30	1	2	5	0.6	0.18

[a]Particle emission indices (PEIs) computed for plume age 3 s and cutoff diameter 5 nm (see Figure 7) for given fuel sulfur content (FSC) to fit volatile particle number concentrations measured with CPCs with cutoff diameter d at plume age t behind the Concorde [*Fahey et al.*, 1995] during SULFUR 5–7 [*Schröder et al.*, 1998, 2000b; *Brock et al.*, 2000; this work], SNIF-II, -III, and SUCCESS [*Anderson et al.*, 1998a, 1998b, 1999b], and POLINAT [*Schumann et al.*, 2000a], using values of EI of condensable organic matter (OM), fuel sulfur conversion fraction (ε), and EI of emitted CIs, for which the model fits the data optimally. Ranges are given for cases with several data. Data as in the work of *Kärcher et al.* [2000], with additions for B737 (S6), B707 (S7), and A340 (S7). The A340 values listed are best estimates; the values in parentheses cover a range of lower and upper estimates. The Concorde values fit the lowest measured PEI of 1.7×10^{17} kg^{-1} at plume ages of 960–3480 s; the model would match PEI values of at most 3.2×10^{17} kg^{-1} in the aged plume for $EI_{OM} = 100$ µg/g, $\varepsilon = 30\%$, and $EI_{CI} = 8 \times 10^{17}$ kg^{-1}.